RESEARCH ARTICLE

BioDiscovery

OPEN ACCESS

The alternate GNB3 splice variant, Gβ3s, exhibits an altered signalling response to EGF stimulation, which leads to enhanced cell migration

Hemanth Tummala[1], Hilal S. Khalil[1], Mohammad R. Islam[2], Sarah J. Jones[2], Ian R. Ellis[2], Isabella D'Ascanio[1], Nikolai Zhelev[1*], Douglas H. Lester[1*]

[1]School of Science, Engineering & Technology, University of Abertay Dundee, Bell Street, Dundee, UK, DD1 1HG
[2]Unit of Cell and Molecular Biology, Dundee Dental School, University of Dundee, Park Place, Dundee, UK, DD1 4HN

Abstract

It has recently been reported that the duplication of the GNB3 gene has been shown to be directly linked to an obesity phenotype, both in humans and also in a humanised mouse model. Moreover, the common human GNB3 c.825C>T polymorphism (rs5443) causes this ubiquitously expressed gene to be aberrantly spliced approximately 50% of the time leading to the production of both a normal Gβ3 protein and a truncated, possibly less stable subunit, known as Gβ3s. The presence of the GNB3 825T allele has previously been shown to be associated with predisposition to hypertension, obesity, various cancers, Alzheimers, age related cognitive function, erectile dysfunction as well as a marker for pharmacogenetic drug action. Great controversy, however, currently exists as to whether these phenotypes associated with the 825T allele are a) mainly due to the presence of the smaller, possibly more active, Gβ3s subunit or b) merely down to the haploinsufficiency of the normal GNB3 transcript, due to its frequent aberrant splicing. In order to try and address these two conflicting hypothesis, we report on the identification and characterisation of signalling alterations unique to the presence of Gβ3s protein subunit. Moreover we also show the physiological consequences associated with altered signalling, directly induced by the Gβ3s subunit. For this, we used both an EBV transformed lymphoblast cell line homozygote for GNB3 825T/825T (TT) and a stable Gβ3s expressing recombinant COS-7 clone. In both of these cell lines that express the Gβ3s subunit, we found enhanced cytosolic calcium influx upon stimulation with EGF, TGFα and VEGF ligands, as compared to "normal" GNB3 controls with the 825C/825C (CC) genotype. This aberrant calcium influx also led to an increase in ERK, but not AKT1, phosphorylation. Despite the lack of AKT1 activation, we paradoxically observed a significant increase in phosphorylation of its downstream substrates, namely mTOR and $p70^{S6k}$ (KS6B2). Moreover we observed a decrease in phospho FoxO3a only in Gβ3s expressing cells, but not in the "normal" GNB3 (CC) control cell line. The presence of the Gβ3s subunit also appeared to alter the distinct localisation patterns of both Foxo3a and AKT1, while also increasing the colocalisation of mTOR and $p70^{S6K}$. Subsequent growth factor stimulation studies revealed that EGF treatment, of Gβ3s expressing cells, appeared to cause a significant decrease in cAMP levels, which, in turn resulted in both enhanced caveolin-1a phosphorylation, and an increase in actin stress fibre formation. The identification of these distinct Gβ3s specific signalling alterations were indicative of a more aggressive migratory phenotype. This led us to further investigate and confirm that the presence of the Gβ3s subunit also appears to cause significantly enhanced migration and robust scratch wound healing kinetics, as compared to cells harbouring only the normal copy of the gene. These data therefore present convincing evidence that the Gβ3s subunit is stable, functional and its presence can significantly alter signalling pathways, in different cell types.

Citation: Tummala H, Khalil HS, Islam MR, Jones S, Ellis IR, D'Ascanio I et al. The alternate GNB3 splice variant, Gβ3s, exhibits an altered signalling response to EGF stimulation, which leads to enhanced cell migration. *Biodiscovery* 2013; **9**: 3; DOI: 10.7750/BioDiscovery.2013.9.3

Received: 8 April 2013; **Revised:** 4 August 2013; **Accepted:** 28 November 2013; **Available online/Published:** 30 November 2013

Keywords: Gβ3s, Calcium, ERK, AKT, cell migration

***Corresponding Authors:** N.Zhelev e-mail: n.zhelev@abertay.ac.uk; D.Lester e-mail: d.lester@abertay.ac.uk

Conflict of Interests: No potential conflict of interest was disclosed by any of the authors.

Introduction

Heterotrimeric G proteins, which consist of an α, β and γ subunit , are involved in signalling pathways which regulate cell migration and chemotaxis both of which are prerequisites for metastasis formation [1]. In humans, 16 different alpha genes encode Gα subunits, 5 different GNB genes encode Gβ subunits (plus additional splice variants) and 12 different GNG genes encode Gγ subunits [2]. Gβγ subunits are involved in the signalling of phosphatidylinositol-phosphates, i.e. phospholipase C (PLC) and PI3 kinase (PI3K), that contribute to regulation of gene expression and tumour cell migration promoting metastasis. Previous studies have shown the involvement of Gβγ signaling in cell migration of endothelial [3] and breast cancer cells [4, 5]. In contrast, Gβγ induced signaling was also shown to inhibit EPAC (RAPGEF3) induced Ca^{2+} elevation and cell migration, *via* additional Ca^{2+} influx from the extracellular space [6]. Moreover, Gβγ signaling was shown to induce PI3K alpha and Src signaling that resulted in downstream activation of AKT and ERK through the Raf, JNK, Ras and Rac pathways. These in turn regulated cell motility, invasion and metastasis [7]. The importance of PI3K pathway in metastasis has previously been demonstrated in cells expressing a "kinase-dead" AKT mutant that resulted in a diminished invasion potential and inability of cells to form tumours or metastasize *in vivo* [8]. Thus, it is clinically important to have a complete understanding of pathways under the regulation of Gβγ subunits and its intracellular effector such as ERK and AKT, which communicate and co-operate between different signaling pathways implicated in critical physiological responses.

Following the original findings of Siffert et al. [9], who first reported the association of the common GNB3 c.825C>T polymorphism with hypertension, we later reported a recessively inherited GNB3 mutation D153del, that causes a retinopathy globe enlarged and a severe renal phenotype in chickens [10, 11].The GNB3 D153delmutation was shown to significantly change the structure of the the Gβ3 subunit, and to alter many downstream effectors controlled by the secondary messengers cGMP and cAMP [10-11]. Such alterations in second messengers have been shown to have a subsequent effect on both the ERK and AKT, components of MAPK and PI3K pathways respectively [11-13].

Interestingly, a recent study has shown that both humans and transgenically engineered mice that carry an extra copy of *GNB3* gene leads to obesity and increased weight and abdominal fat content in humans and mice respectively [14]. The common human polymorphic variant 825C>T in exon 10 of the *GNB3* gene causes its transcript to missplice at a cryptic splice site in exon 9, in approximately half of all transcripts produced. This smaller transcript is translated into an immunologically detectable truncated, smaller Gβ3 (Gβ3s) protein subunit [9]. It has been hypothesized that this Gβ3s protein subunit forms a 6 as opposed to the normal 7 WD propeller structure [9]. The presence of the Gβ3s subunit, in GNB3 825T cells, appears to cause hyperactivating gain in function and signalling activity, in the few cell types that have been studied [e.g. 9, 15-17]. As the 825T allele is found in approximately half of all human chromosomes by deduction the Gβ3s subunit is therefore also expressed in approximately half of the world's population. The 825T allele and also the Gβ3s subunit has been recognised as a predisposing factor for common diseases such as hypertension, Alzheimer's disease, major depressive disorder, obesity, and coronary heart disease [reviewed in 18].

A previous cohort study in cancer patients with transitional cell bladder carcinoma reported that the GNB3 825T polymorphism influenced the biological behaviour of tumour disease [19]. This study revealed a shorter time for metastasis in 825T-allele carriers compared to individuals that were homozygous for the GNB3 825C allele. In subsequent studies, it was found that individuals who were suffering from either oncocytic thyroid tumours, head and neck squamous cell carcinoma or bladder carcinoma, were at a significantly higher risk for tumour relapse and death when they were homozygous for the GNB3 825T allele [20, 21]. On the contrary, a different study found that the GNB3 825T allele appears to be protective against the development of bone metastasis in breast cancer patients when compared to individuals homozygous for the 825C allele [22]. These results demonstrate that the expression of the variant Gβ3s protein, in different cell types can have different signalling outcomes causing different physiological effects. However the underlying signalling mechanisms that lead to such a plethora of different phenotypic alterations, are far from being fully elucidated, for the GNB3 825T allele.

Therefore understanding the effects of the splice variant Gβ3s protein subunit, in the Gβγ signalling pathway, may help us explain the complex disorders that 825T GNB3 individuals are predisposed to. However, due to the limited access to affected human tissues, currently only appropriate cellular models can be employed to decipher such signalling changes. B-lymphoblast cells, however, have previously been used as a convenient experimental cell system, that has led to the reproducible assessment and examination of complex molecular signaling networks [23]. Moreover the convenient use of EBV transformed B lymphoblast cells, as a model to study basic molecular mechanisms and genetic associations of human diseases, is becoming increasingly widespread [24-27]. The application of this model to explore cell signaling

and physiology patterns seems particularly appropriate given that these cells share many common molecular and cellular features important for cell signaling for instance, those that relate to cell motility and morphology. For example lymphoblast cell lines have previously been used for cell migration studies to understand neural cell motility, which plays a significant role in schizophrenia [24].

Controversy exists in whether the presence of Gβ3s causes any signaling alterations unique to this truncated form leading to functional consequences, or if it is functionally unstable. For example, Virchow S et al reported that neutrophils of homozygous GNB3 (TT) genotype displayed enhanced migration kinetics as compared to neutrophils of heterozygous GNB3 825C/825T (CT) and homozygous GNB3 (CC) genotype [12]. On the contrary, a recent study claimed that this variant is an unstable protein and functionally inactive [28]. In order to identify whether the Gβ3s subunit is indeed both stable and functional we firstly used EBV transformed human B lymphoblasts homozygous for either the 825C or the 825T alleles. The former cell line expresses only Gβ3, while the latter cell line expresses approximately equal amounts of both Gβ3 and Gβ3s subunits. Secondly we also generated a stable COS-7 clones expressing either a 6xHis tagged Gβ3 normal (Gβ3-COS) or Gβ3s mutant subunit (Gβ3s-COS). From experiments with these cell lines, our findings indicate that the Gβ3s is indeed both stable and functionally active. For example following growth factor stimulation of our cell lines, the presence of Gβ3s shows a significant rise in enhanced cytosolic Ca^{+} influx, causing an activation of ERK and repression of AKT phosphorylation. This in turn leads to a decrease in cAMP levels causing subsequent Caveolin 1a (Cav1) phosphorylation. These signalling events induced cytoskeletal remodelling leading to actin stress fiber formation and overall enhanced cell migration and scratch wound healing ability, that were unique to Gβ3s containing cells and absent in cells containing the full length Gβ3. Thus we illustrate a novel signaling mechanism induced by Gβ3s following growth factor stimulation that results in more aggressive migratory phenotype.

Materials and Methods

Cell culture and treatments

Immortalised B-lymphoblast cell lines expressing 825CC (GM19116) Gβ3 and 825TT (GM18500) Gβ3s protein were obtained from Coriell Cell Repositories, USA. These cell lines were cultured in 10% FCS supplemented RPMI media (Invitrogen UK) in culture flasks. Simian COS-7 cells (ATCC CRL 1651) were maintained in DMEM (Invitrogen, UK) supplemented with 10% foetal bovine serum (FBS), 2 mM glutamine, 1 mM sodium pyruvate, 100 µg/ml streptomycin and 100U/ml penicillin in an atmosphere of 5% CO_2. Cells were stimulated with Epidermal Growth Factor (EGF) or Transforming Growth Factor alpha (TGFα) or Vascular Endothelial Growth Factor (VEGF) (Invitrogen, UK). Treatments with inhibitors were performed with Verapamil, a calcium channel blocker at 20µg/ml [83], U0216, a dual MEK1 and MEK2 inhibitor at 25mmol/ liter [84], and GRK2i peptide [85] (Tocris UK) for 2 hrs in DMEM containing 1% serum. The specificity of each inhibitor treatment was evaluated by monitoring their functional activity (see Results). Cell viability was >90% for each inhibitor treatment as judged by trypan blue staining (Data not shown). Forskolin (Fsk) was purchased from Sigma Aldrich UK.

Plasmids, transfections and stable clones

Both (pCDNA 3.0) His tagged GNB3 and GNB3s were constructed by PCR amplification of pREP4-GNB3 and pREP4-GNB3s cDNAs obtained from Dr. M.J Bullido (Universidad Autónoma de Madrid, Cantoblanco, Madrid, Spain) using primers carrying flanking restriction sites forward HindIII, 6x His tag (underlined) 5'AAGCTTATGCATCATCACCATCACCACACGG GGAGATGGAGCAACTG 3' and reverse XhoI sites 5' CTCGAGTCAGGTTCCAGATTTTAGG 3'. PCR amplified fragments were digested and sub-cloned into pCDNA3.0. The fidelity of the constructs has been checked and verified by sequencing using a commercial sequencing service (www.dnaseq.co.uk). COS-7 cells were transfected using electroporation. When they reached confluence at 2 x 10^7, cells were washed in PBS and resuspended in 400µl of the Optimem transfection media (Invitogen UK), and were electroporated using settings at 400V, 350µF, using Easyject EquiBio (Kent UK). 10µg DNA was used per transfection. Subsequently, stable clones expressing 6xHis-tagged Gβ3 (Gβ3-COS) and Gβ3s (Gβ3s-COS) were generated by selection with G418 (Invitrogen UK) at 800 µg/ml, and subsequently maintained at 400 µg/ml. The culture was placed back in the incubator until individual colonies were visible. Individual colonies were expanded, and the level of 6x Histidine-tagged Gβ3 and Gβ3s protein expression was determined by western blot analysis using anti-His antibody mentioned in Table 1.

Antibodies, immune-blotting and data presentation

Expression of Gβ3 and Gβ3s protein was detected using Anti- rabbit GNB3, anti-sera on B lymphoblast cells at a relevant dilution (1:2000) in blocking reagent. The antibodies mentioned in table 1 are used to detect the expression of phosphorylated and total proteins levels in B lymphoblast cell lysates. Rho A, Rho B, Rho C, Rac

Table 1. Antibodies used in the study.

Antibody	Company
GNB3	EURGENE TECH
MAPK (ab17942)	Abcam
Phospho-MAPK (ab50011)	Abcam
FoX03a (2497)	CST
Phospho-FoX03a (9465)	CST
ATK (9272)	CST
Phospho-AKT (S473)	CST
Phospho-AKT (T308)	CST
mTOR (2972)	CST
Phospho-mTOR (S2871)	CST
β-Actin (ab1801)	Abcam
Phospho-Caveolae-1 (ab38468)	Abcam
4E-BP1 (9451)	CST
Phospho-4E-BP1 (T46)	CST

1-2-3 and CDC42 total and phosphorylated expression were determined using Rho GTPase antibody sampler kit (Cell signalling, UK). Briefly, by centrifuging cells at 1500g for 5min, the obtained pellet was washed twice with ice cold PBS and centrifuged again at 1500g for 5 min. 1 ml of RIPA buffer (Pierce Biotechnology UK) was added to 40 mg of wet cell pellet, mixed well and then sonicated for two cycles of 5 seconds at 50% pulse. The final mixture was shaken gently on ice for 15 min and the protein supernatant was obtained by centrifuging the cells at 14000g for 15 min. Subsequently all protein extract samples were quantified with the use of a spectrophotometer, with BSA as a standard. 50µg cell lysates were mixed with sample buffer and equal concentrations were loaded on 10–12% SDS–polyacrylamide gels. After electrophoresis, the proteins were transferred to nitrocellulose membranes (Bio-Rad Hybond ECL). Further blotting was carried out using a commercially available kit (QDOT® 625 Streptavidin conjugate kit, Invitrogen, UK). Non-specific reactivity was blocked by incubation with a blocking reagent supplied in the kit. Membranes were further processed by incubating them with relevant primary antibodies described in Table 1, washed and further incubated for an hour (hr) with Biotin labelled secondary antibodies. Finally, bands were visualized with the enhanced streptavidin substrate, washed and visualised under the UVDOC imaging system (Alpha Innotech). For internal control, the levels of β-actin were examined on the same blot by incubating the blots with stripping solution for 1 hr (20% SDS, 67.5µM Tris-HCl of a pH 6.7, 100µm 2- Marcaptoethanol) and reprobing with anti-β-actin (Sigma-Aldrich, UK) and anti-mouse IgG secondary antibody (Sigma-Aldrich, UK). Densitometry analyses on the immunoblotted images were performed by Gelpro software (Media Cybernetics, USA). Statistical analysis was performed using Graph Pad Prism (USA) and displayed as mean ± S.E. The significance (p value) of differences of pooled results was estimated by '*t*' tests, and were defined as *p< 0.05.

FITC conjugated cholera toxin B (CTB) uptake, Immunocytochemistry (ICC), imaging and co-localisation

Stable expressing His-Gβ3 and His-Gβ3s COS cells were grown on standard glass coverslips coated with polylysine (Sigma-Aldrich, UK). They were placed in petri dishes containing Dulbecco's modified Eagle's medium (DMEM, Invitrogen, UK) supplemented with 10% fetal bovine serum and allowed to grow for 18-24hrs. Following relevant treatments, cells were fixed in 3% paraformaldehyde in a standard PBS at room temperature for 30 minutes (min). The cells were then gently washed twice with 1 ml of PBS, and blocked using 1% goat serum and 1% bovine serum albumin in PBS containing 0.05% Triton X-100, for 30 min. They were then incubated with a primary antibody diluted in blocking solution for 30 min, washed three times with the 0.3% Triton X-100/ PBS for 5 min, and then incubated with the relevant Alexa fluor 488 and Alexa Flour 568 conjugated goat anti-rabbit secondary antibodies (Invitrogen UK) for 30 mins. Fluorescent Alexa Fluor 568 phalloidin (Invitrogen UK) was used to visualize actin structures. For nuclear staining, cells were mounted with DAPI containing Vectashield solution (Vector Laboratories UK). Cells showing actin filament bundles across cell bodies were counted as stress fiber positive, cells showing mainly cortically distributed actin filaments were counted as stress fiber negative. Mounted cells were imaged under a Leica DMiRe2 electronic controlled microscope, under relevant excitation and emission filters depending on the fluorotype. An iXonEM +897 EMCCD camera (ANDOR technologies ltd, USA) was used to capture images and visualisation was performed using multi-dimensional microscopy software Andor Module iQ Core. Colocalisation assays were performed and determined with software integral features supplied by Andor IQ core software features.

Migration assay

Migration assay was performed using the 48-well Boyden chambers (8 µm pores, BD Biosciences). The

cells were plated at a density of 1 × 10^6 cells/100 µl serum-free media containing 10% BSA which was used as a positive control. This was placed in the bottom wells of a Boyden chamber. A medium containing lymphoblast cells, starved for 2 hr in serum free media, was added to the top chamber. For the inhibition assays, cells were starved for 2 hr and pre-incubated with inhibitors for 30 min. Inhibitors were also added to the cell suspension placed on the top chamber wells, and also to the chemoattractant added to the bottom chamber wells, in order to be present during the migration time. After 6 hr incubation the cells were stained using the Diff-Quick kit (Dade Behring). Pictures were taken with a light microscope and migrated cells were counted with Gelpro Software (Media cybernetics, USA) using 10 randomly chosen fields.

Calcium influx assay

Lymphoblast cells at 125000 cells / well density were plated in a 96 well plate and incubated for 16hrs in RPMI media (Invitrogen UK). 16 hrs later RPMI media without serum was added prior to stimulation with EGF. Upon EGF stimulation at relevant time points, cytosolic calcium influx assay was carried out using Molecular Probes' Fluo-4 NW (No-Wash) Calcium Assay Kit (Invitrogen UK) following the kit instructions. Calcium response was detected using the Modulus™ Microplate Multimode Reader plate reader using instrument settings appropriate for excitation at 494 nm and emission at 516 nm. Functional parameters were determined with Graph Pad PRISM software using non-linear regression applied to a sigmoidal dose response model.

cAMP assay

cAMP assays were carried out as mentioned in Tummala et al 2011 [11] to detect variations in the concentration levels of cAMP upon EGF induction at indicated time points in the B lymphoblasts. Briefly, the protein extracts acquired from B lymphoblast and COS-7 stable clones were acetylated following the kit instructions (Cayman Biosciences) to increase the sensitivity of detection. For cyclic nucleotide determination, protein samples are diluted with 0.1 M HCl that inactivates phosphodiesterases and lower the concentration of immunoglobulins that may interfere with the assay. 10 µg/well concentration of protein lysates were loaded on a 96 well plate, and the assay was carried out as detailed in the kit instructions. The enzymatic reaction was stopped after incubation using reagent supplied in the kit, and the resulting yellow colour was read on a colorimetric microplate reader at 405 nm (Anthos HTIII Microplate Reader, Denley Instruments, UK). The optical density of the bound colour emitted is inversely proportional to the concentration of cAMP level in samples, which was calculated according to the instructions supplied in the kit. All results were analysed by oneway ANOVA with posthoc Dunnett tests using the GraphPad Prism 3.02 software. Data was generally expressed as mean 6 S.E.M. for individual sets of experiments.

Scratch wound assays

Stable COS-7 clones expressing His-Gβ3 and His-Gβ3s subunits were plated onto poly-d-lysine-coated coverslips (10 µg/ml). These were grown to 100% confluence, and serum starved for 12hr. Wounds were created by scraping the monolayer of cells with a sterile pipette tip and culture media was added with or without inhibitors. The images of wounds were captured at 5x magnification with a Leica DMiRe2 electronic controlled microscope immediately after wounding and again 24 h later. Images were collected under bright field using an iXonEM +897 EMCCD camera (ANDOR technologies ltd, USA) and visualised using multi-dimensional microscopy software, Andor Module iQ Core. The images were subjected to the WIMASIS image analysis application that is available for use on the Wimasis my Wim platform. The data is presented as cell covered area at noted time points and estimates the effects of inhibitors on cell migration.

Results

Expression and characterisation of Gβ3s subunit

EBV transformed Gβ3 expressing lymphoblastoid cells (CC) and Gβ3s/Gβ3 expressing lymphoblastoid cells (TT) were grown in relevant media, harvested and lysed to obtain protein lysates. Following processing of the lysates for immunoblotting, SDS-PAGE was performed and the blot was probed with a custom raised Gβ3 specific antibody [11]. The fundamental difference between CC and TT lymphablastoid cells was the expression of only the larger "normal" 340 amino acid long Gβ3 protein (calculated Mol. Wt. = 37090 Daltons) in the CC cell line while the latter, TT cell line expressing approximately equal quantities of both the Gβ protein and the smaller 299 amino acid Gβ3s protein (calculated Mol. Wt. = 34990 Daltons) (figure 1a). Protein lysates obtained from COS-7 clones following stable transfection with either histidine (His) tagged Gβ3 construct (Gβ3-COS) or His tagged Gβ3s (Gβ3s-COS), when probed with anti His antibody, revealed similar expression pattern, with His-Gβ3s producing a lower band when compared to His-Gβ3 protein (figure 1b). G-proteins are highly expressed in the endomembrane and Golgi vesicle compartments and display diffused transport kinetics upon stimulation [27]. Following immunostaining of Gβ3-COS and Gβ3s-COS with anti-His antibody, similar subcellular expression was observed for Gβ3 and Gβ3s with both showing co-localisation with the co-transfected Golgi-YFP (figure 1c-d).

It has been known that in culture cells, Gβ and Gγ subunits interact to rapidly form the irreversible Gβγ dimer following synthesis [29]. Cell periphery staining of Gβ3 and Gβ3s was observed that indicated their plasma membrane association along with endogenous Gγ subunits, expressed as Gβγ dimers. This observation suggests that our stable clones express the His tagged constructs of Gβ3 and Gβ3s subunit that can efficiently form dimer with endogenous Gγ, and get processed as Gβγ dimer, to traffic between cytosol, Golgi and plasma membrane.

Epidermal Growth Factor (EGF)-induced Ca^{2+} ion influx was enhanced in the presence of Gβ3s

Intracellular Ca^{+} ions are known to be modulated following G-Protein Coupled Receptors (GPCRs) stimulation via Gβγ [30]. Moreover Gβγ signaling and Ca^{2+} mobilisation both co-operate synergistically in the activation of JNK by Gq-coupled receptors [30]. Hence, we wanted to examine whether stimulation with EGF will cause any change in the Ca^{+} ion influx in our cell line models and also whether this Ca^{+} response will be altered due to the presence of Gβ3s subunit instead of its normal counterpart. To determine this, we exposed TT and CC lymphoblastoid cell line models to EGF. Growth factor stimulation significantly increased Ca^{+} ion influx in both cell lines (figure 2). However, there was significantly greater initial increase in TT cells compared to CC cells. Moreover, while there was some degree of time dependent fluctuation of Ca^{+} ion influx, the TT cell line sustained this enhanced in flux over the course of 200 seconds (figure 2). This study indicated Gβ3s dependent signaling alteration and provided first functional evidence in the current investigation that was specific to the Gβ3s subunit.

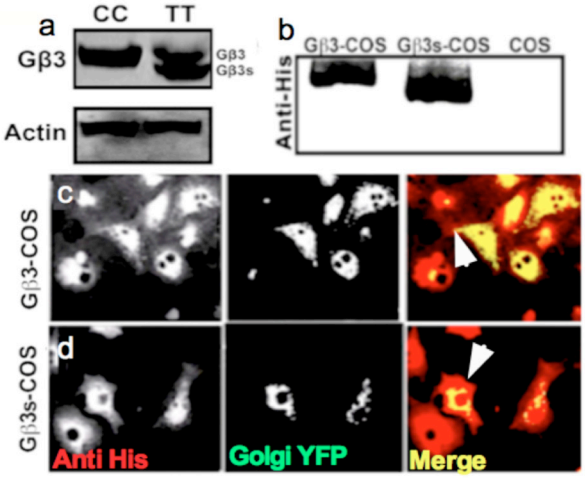

Figure 1. Expression of Gβ3 and Gβ3s subunits. CC and TT lymphoblast cell lysates were immuno blotted with custom raised GNB3 antibody to determine Gβ3 and Gβ3s protein expression levels respectively (a). Protein lysates forming stable COS-7 clones were analyzed for the expression of His tagged Gβ3 and Gβ3s upon immunoblotting with Anti-Histidine (his) antibody (b). Data presented here is of n = 3 independent experiments. No localisation difference between His tagged Gβ3s and Gβ3 subunit was observed when immune probed with Anti-his in stable clones transfected with Golgi-YFP in both untreated and EGF stimulated condition (c-d). These images are taken from different fields of view under a 40x objective with further 1.5x magnification.

Gβ3s induces ERK activity and activates mTOR pathway but not AKT1

MAPK cascades are evolutionarily conserved in regulating cell signal transduction by connecting cell-surface receptors to critical regulatory targets within cells. These pathways are essential in controlling cell survival, proliferation and apoptosis. Since both Receptor tyrosine kinases as well as GPCRs signal mainly via PI3K and MAPK pathways, we wanted to determine whether the presence of Gβ3s will have any impact on the key effector proteins of these pathways. We found that both TT lymphoblastoid and Gβ3s-COS cells had significantly higher basal levels of ERK phosphorylation (figure 3 a). Probing for the presence of phosphorylated AKT1 on the contrary revealed a reduction in basal Threonine-308 (T-308) and Serine-476 (S-473) AKT1 phosphorylation in both TT lymphoblastoid and Gβ3s-COS cells as compared to their normal counterparts (figure 3a and 3g). Interestingly, both TT lymphoblastoids and Gβ3s-COS also showed enhanced mTOR phosphorylation at Serine 2481 (S-2481) despite the reduction in AKT1 phosphorylation (figure 3b). This prompted us to look at downstream phospho induction of mTOR substrates. As shown in figure 3b, enhanced mTOR phosphorylation was also accompanied by induction of its substrates $p70^{S6K}$ [phospho Threonine 389 (T-389) and phospho Serine 371 (S-371)] and 4E-BP1 [phospho Threonine 46 (T-46)] indicating hyperactivation of mTOR pathway in Gβ3s containing cell lines.

Previous studies have reported that agonists of GPCRs potentiate the mitogenic effect by promoting a sustained late phase activation of PI3K and $p70^{S6K}$ via a pathway dependent on the Gβγ subunits of heterotrimeric G proteins [31]. The activation of $p70^{S6K}$ is a critical step in ribosomal biosynthesis promoting translational activation within a cell [32]. Phosphorylation of particularly S-371 residue of $p70^{S6K}$ has been shown to be a specific target of mTOR in breast cancer cells [33]. Our results suggest that in the presence of Gβ3s, there was upregulation of $p70^{S6k}$ activity and 4E-BP1 probably in mTOR dependent manner but independently of PI3K and AKT, which may implicate increased translation in Gβ3s containing cells.

Gβ3s promotes nuclear accumulation of Foxo3a suggesting an increase in its transcriptional activity

AKT activation leads to phosphorylation of Foxo3a that results in its exclusion from nucleus and sequestration

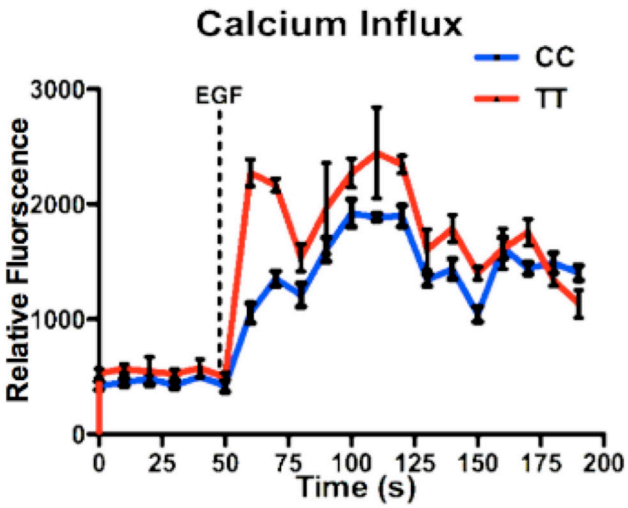

Figure 2. Gβ3s subunit leads to enhanced Ca^{2+} influx kinetics. Intracellular cytosolic Ca^{2+} influx was quantified using Fluo-4 NW as mentioned in materials and methods. Ca^{2+} quantification assay revealed enhanced Ca^{2+} influx in TT lymphoblast upon EGF stimulation, when compared to CC lymphoblast cells. Data presented in all panels are the mean with standard error (bars) of n = 3 independent experiments performed in octuplets. Statistical significance is shown as *P<0.05, **P<0.01, ***P<0.001.

in cytoplasm, thereby inhibiting its transcriptional function [34]. Since we found downregulation of AKT activity in our cell line models, we next asked whether this downregulation would also result in reduction of phospho Foxo3a, which would then lead to its nuclear accumulation allowing it to functions as a transcription factor. Also, the fact that we saw elevated $p70^{S6k}$ in the presence of the Gβ3s variant, indicating translational induction, we wanted to see whether the presence of Gβ3s would similarly cause transcriptional induction via Foxo3a activity. According to figure 3b, there was a significant reduction in phosphorylated levels of Foxo3a on Serine 318/321(S-318/321) and Serine 253 (S-253) indicating its activation.

Immunostaining of subcellular Foxo3a revealed that Gβ3s induced reduction of phospho Foxo3a also led to an increase in its nuclear accumulation in constitutive state (figure 3 e & j) as well as following stimulation with EGF (figure 3 f & k) in our cell line models. This particular nuclear staining appears to be absent in CC lymphoblast (figure 3c-d) and Gβ3-COS cells (figure 3h-i) expressing normal Gβ3 subunit. These figures suggest that loss of AKT phosphorylation in the presence of Gβ3s may lead to Foxo3a mediated transcriptional induction and hence present an altered signaling profile as compared to cells harboring the normal copy of the gene.

Presence of Gβ3s variant causes downregulation of Cyclic AMP and increased phosphorylation of Caveolin 1a in response to EGF stimulation

Gβγ signaling has been shown to play a role in modulating intracellular levels of second messenger, cyclic AMP (c-AMP) and its function has been implicated in both c-AMP increase [35] and decrease [36]. Furthermore, c-AMP was previously found to inhibit MAPK levels via its activation of Protein kinase A (PKA) that resulted in repression of ERK phosphorylation [37]. This prompted us to investigate the effect of Gβ3s on c-AMP levels and also determine whether the enhanced ERK phosphorylation due the presence of Gβ3s seen in figure 3 (b & g) may also be contributed by modulation of c-AMP levels. Following treatment with c-AMP inducer Forskolin, higher levels of cAMP generation was observed in TT cells as compared to CC. Contrastingly, upon EGF stimulation, cAMP levels were found to be downregulated in TT lymphoblast cells as compared to CC (figure 4a).

Altered cAMP regulation in TT lymphoblastoid cell line can implicate differences in various signaling processes including differential regulation of the microenvironment by recruitment of scaffolding molecules that include caveolae [38]. Hence, we next investigated any changes in caveolin 1 (Cav 1), an essential component of caveolae, which are a subtype of cholesterol-enriched lipid microdomains/rafts. Investigation of Cav1 levels were based on the following reasons: Firstly, Gβγ signaling has been shown to modulate caveolae function [39], secondly, Foxo3a transcription factor, which in this study was found to be stabilized in the nucleus, was previously shown to transcriptionally upregulate Cav1 [40] and lastly the c-AMP levels, which were shown to drop in Gβ3s containing cell lines, were reported to downregulate Caveolin-1 expression [41].

These previous reports as well as insights from current investigation led us to propose that the phosphorylated levels of pCav1 might be altered in Gβ3s containing cells as compared to their normal counterparts. Indeed we found that both at basal levels and upon EGF stimulation, the levels of phosphorylated Cav1 at tyrosine 14 (Y-14) residue in both Gβ3s-COS and TT lymphoblast cells showed an induction in comparison to Gβ3-COS and CC lymphoblast cells respectively (figure 4b) thus confirming our hypothesis. These studies also suggest that Gβ3s signaling may be involved in cytoskeletal remodeling and maintenance of cell shape, features that regulate cell migration and metastasis, by modulating c-AMP levels that result in changes in Caveolae microdomains.

AKT1 localisation towards caveolar membrane free domains is reduced in the presence of Gβ3s subunit

Following the previous finding that Cav1 phosphorylation was enhanced in Gβ3s containing cells, we next wanted to determine at a cellular level whether there is an accompanying altered localisation of substrates of PI3K

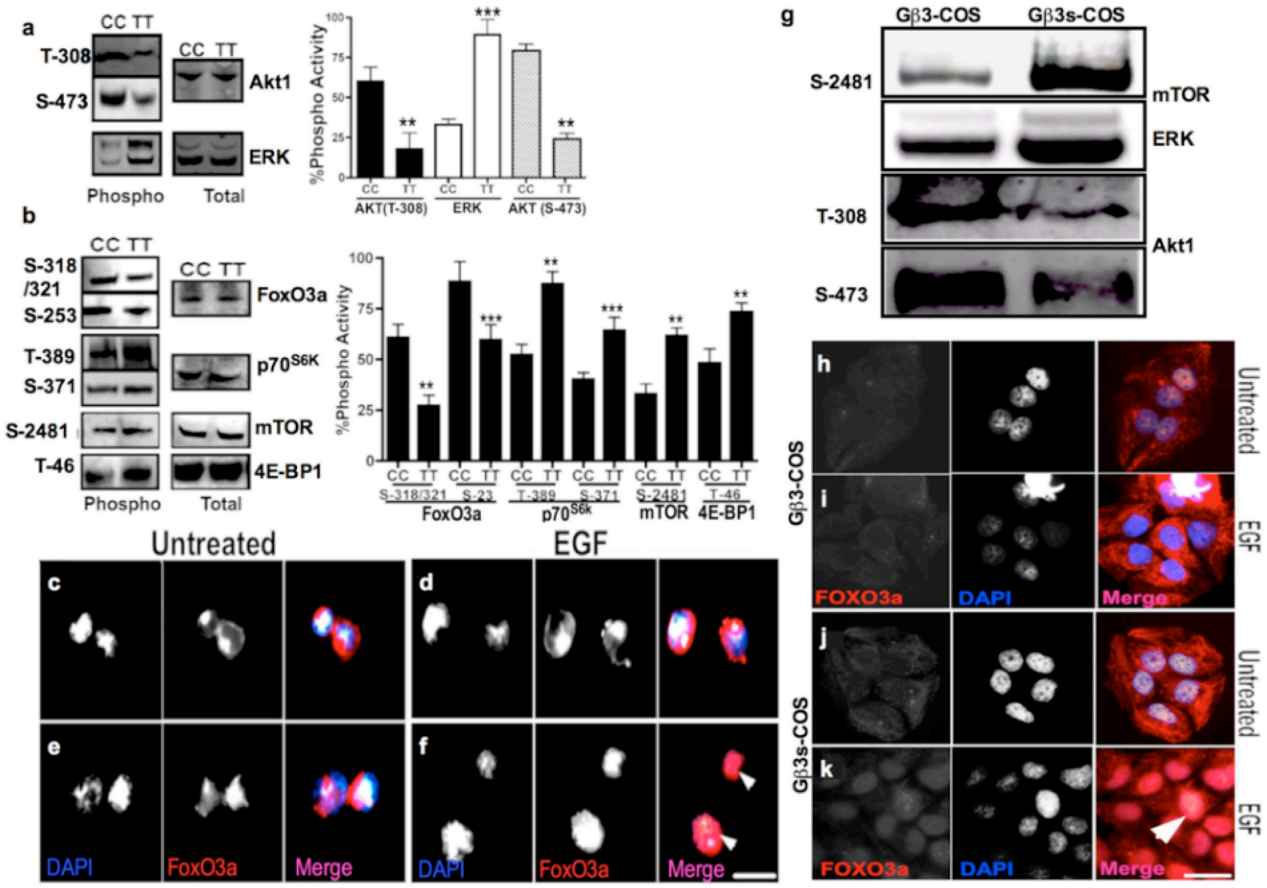

Figure 3. Gβ3s subunit hyper activates ERK overcompensating for the lack of AKT activity. Phospho immuno reactivity of ERK2 and AKT1 at relevant residues are shown in CC and TT lymphoblast protein extracts (a). TT lymphoblast protein extracts showed significant changes in relative phosphorylation activity when compared to CC lymphoblasts in PI3K-AKT pathway substrates such as Foxo3a, mTOR, $p70^{S6k}$ and 4E-BP1 at relevant residues (b) which was confirmed by semi quantitative densitometry analyses as described in materials and methods. Data presented in all panels are the mean with standard error (bars) of n = 3 independent experiments. Lysates from stable COS-7 clones showed similar kinetics in terms of ERK and AKT1 phosphorylation as observed in lymphoblastoid cells (g). Statistical significance is shown as *P<0.05, **P<0.01, ***P<0.001. Foxo3a immuno staining of lymphoblast cells was performed using total Foxo3a antibody at both basal and EGF stimulated condition as mentioned in methods (c-f). TT lymphoblast cells and Gβ3s-COS7 cell showed distinct nuclear Foxo3a staining. White arrows indicate co-localisation with DAPI (blue) upon EGF stimulation confirming nuclear retention (f & k). This particular nuclear staining was not observed in CC lymphoblasts and Gβ3-COS cells both in untreated (c & h) and EGF stimulated conditions (d & i). Images were taken from different fields of view under a 40x objective with further 1.5x magnification. Bar = 13μm.

pathway at caveolae. This was done owing to the fact that we had found altered phosphorylated levels of PI3K substrates that can lead to a substantial change in their sub-cellular compartmentalisation.

Monitoring the cholera toxin B (CTB) subunit internalisation in mammalian cells has previously been reported as a marker for uptake via the caveolae-dependent pathways [39]. We used Fluorescein isothiocyanate (FITC) conjugated CTB subunit (FITC-CTB) to study the localisation of AKT, mTOR and $P70^{S6K}$ within caveolae at a single cell level both in Gβ3-COS and Gβ3s-COS cells at basal levels and following EGF stimulation. In Gβ3-COS cells, we found co-localisation of AKT1 with internalized caveolae both in untreated states and following EGF stimulation (figure 5a, a', b & b'). Interestingly, this co-localisation of AKT1 and caveolae was disrupted in Gβ3s-COS cells both in untreated and following EGF stimulated states (figure 5 c, c', d, d'). This suggested that reduced levels of phospho AKT1 found in Gβ3s caused mislocalisation and failure of total AKT levels to localise with internalized caveolae. This finding led us to extend our cell staining study and investigate whether the enhanced phosphorylated forms of mTOR and $P70^{S6K}$ observed in Gβ3s containing cells would cause their increased localisation with caveolae. Immunostaining of mTOR and $P70^{S6K}$ in individual cells and their co-localisation with FITC-CTB revealed enhanced co-localisation between the two in untreated Gβ3s-COS cells and exhibited a further induction following EGF stimulation (figure 5 g' and h' for mTOR staining and k' and l' for $P70^{S6K}$). On the other hand, Gβ3-COS cells exhibited such co-localisation only following EGF stimulation and failed to show any co-localisation in unstimulated condition (figure 5 e' and f' for mTOR and i'

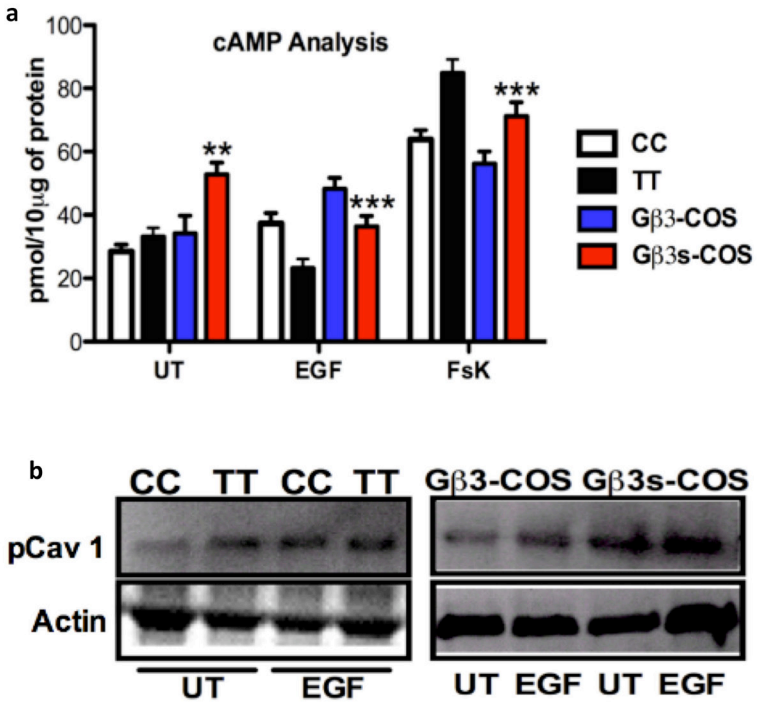

Figure 4. Lack of cAMP induces caveolar-1a phosphorylation. cAMP analysis was measured in CC and TT lymphoblast protein lysates obtained from either untreated cells, or following treatments with EGF or Forskolin (Fsk) as mentioned in methods (a). Decrease in cAMP generation upon EGF stimulation in TT lymphoblast leads to increased phosphorylation of Cav -1a when compared to CC lymphoblast cells (b). Similar trend in cav-1a phosphorylation kinetics was observed in COS-7 stable clones. Data are the mean with standard error (bars) of n=3 independent experiments. Statistical significance is shown as *P<0.05, **P<0.01, ***P<0.001.

and j' for $P70^{S6K}$). This difference between Gβ3 and Gβ3s mediated signaling could have important implications. PI3K is an upstream activator of AKT that operates by recruiting AKT to cellular membranes via the pleckstrin homology membrane-binding domain of AKT. It has been shown that membrane-microdomain compartmentalisation is critical for maintaining proper PI3K/AKT signaling in response to insulin and dysregulating raft-localised PI3K/AKT signaling [42]. Lack of AKT1 at the membrane in Gb3s-COS cells implies that the decrease in activation of AKT1 (figure 3a & 3g) might have affected its membrane-binding dynamics resulting in the absence of a fully functional AKT1at the cell membrane (figure 5 c' & d'). On the other hand, increased signaling activity and localisation of mTOR, $p70^{S6K}$ but not AKT1 to caveolae structures (figure 6 g' & h') suggests that Gβ3s subunit signaling primarily uses caveolae as localised signaling domains that may promote cytoskeletal remodeling and actin reorganisation, features that may induce cell migration and metastatic behavior.

Gβ3s subunit localises in and enhances actin stress fibers formation

The cell cytoskeleton is a network of structural fibers found within the cytoplasm of a cell. It is responsible for cell movement and shape stability. Actin microfilaments are one of the three major types of fibers that form the cell cytoskeleton. Through their association with motor proteins such as myosin, actin microfilaments carry out cellular movements [43]. Discoveries made in the previous section i.e. Cav1 Y-14 phosphorylation was induced in Gβ3s cells both in basal and EGF stimulated states as well as the localisational differences of AKT, mTOR and $p70^{S6K}$ with caveolae between Gβ3 and Gβ3s expressing cells, prompted us to study any changes in the cell cytoskeleton in cells carrying Gβ3s subunit. Investigating cytoskeletal changes were also based on the fact that Cav-1 was found to be associated with actin fibers through induction of cross-linking of filamin protein [44]. Additionally, Gβγ signaling is known to activate PAK1/PIX alpha/Cdc42 pathway for the localisation of F-actin at leading edge of cell for directional sensing, and the persistent directional migration of chemotactic leukocytes [45]. We found that following fluorophore conjugated phalloidin staining and counting the number of F-actin fibers per cell, Gβ3s-COS cells displayed enhanced basal as well as EGF induced F-actin stress fiber formation as compared to normal Gβ3-COS cells (figure 6 a-e). Moreover, immunolabelling of phalloidin-stained Gβ3-COS and Gβ3s-COS cells with anti His antibody revealed enhanced co-localisation between Gβ3s and actin stress fibers both at basal and EGF induced states as compared to cells with Gβ3 (figure 6 f-i). This implies that Gβ3s subunit may participate in F-actin filament

assembly and formation of stress fibers not just by down regulation of c-AMP and upregulation of Foxo3a leading to activation of Cav1a as illustrated in previous sections, but also via direct binding to actin filaments that may recruit scaffolding and structural proteins with enhanced kinetics.

Actin reorganisation and modeling, which is a key element in cell migration, has previously been shown to be in part dependent on PI3K and Ras pathway, independent of GPCRs, where PI3K was found to localise at sites of F-actin projection [46]. Recently, regulation of F-actin assembly was also reported in PI3K independent but AKT dependent manner [47] while earlier reports have demonstrated that activation of $P70^{S6K}$ alone was sufficient for F-Actin remodeling and cell migration even in the presence of PI3K inhibitors [48]. Since in the presence of Gβ3s, phosphorylated levels of AKT1 were downregulated even though cells exhibited F-actin stress fiber formation, we next asked whether the upregulated levels of mTOR and $P70^{S6K}$ were localised at the F-actin assembly in the Gβ3s cells and hence implicate their involvement in cytoskeletal remodeling in the absence of any phospho ATK. We found that AKT1 failed to co-localise with F-actin stress fibers in the EGF treated Gβ3s-COS cells (figure 7, compare a & b with c & d). Interestingly, enhanced co-localisation of mTOR and $p70^{S6K}$ within F-actin stress fibers was observed in Gβ3s-COS cells (figure 7g, h, k & i) when compared to Gβ3-COS (figure 7e, f, j & l). This suggests that these molecules interact specifically within the stress fiber region to regulate cytoskeletal remodeling and perhaps alter cell motility.

The altered localisation of total AKT in Gβ3s-COS cells at both basal and EGF stimulated conditions indicate that the reduced AKT S-473 and T-308 phosphorylation in TT lymphoblast and Gβ3s-COS cells (figure 2a & 3g), impaired its co-localisation with actin filament assembly.

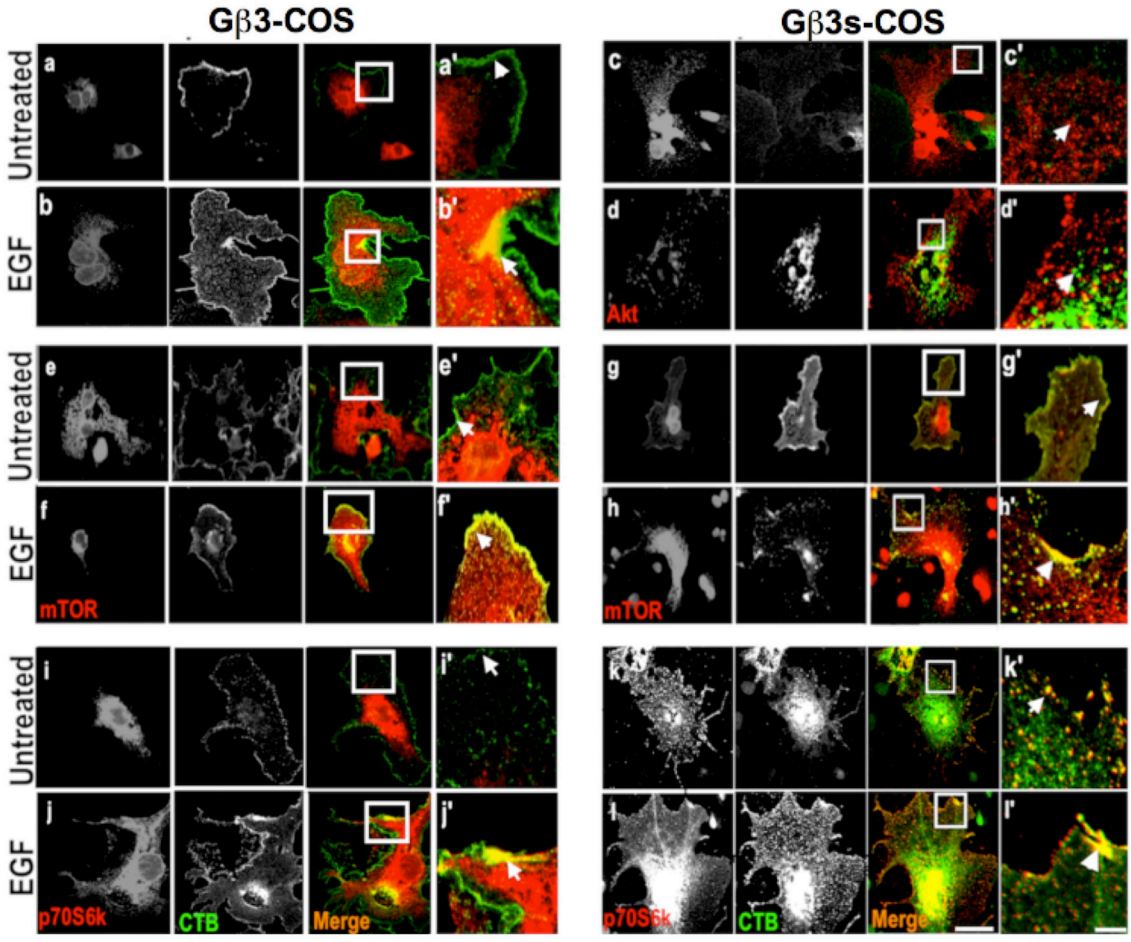

Figure 5. Gβ3s containing cells exhibit enhanced co-localisation of mTOR and $p70^{S6K}$ with caveolae while mislocalisation of AKT. Cholera toxin B (CTB) subunit uptake studies were performed in Gβ3-COS and Gβ3s-COS cells upon EGF stimulation. Cells were treated with CTB for 2 hr and stimulated with EGF, fixed and co-immunostained with AKT, mTOR and $p70^{S6K}$ antibodies and secondary antibodies conjugated to Alexa Flour 568. Gβ3s-COS cells lack co-localisation of AKT with CTB-FITC (c & d with highlighted boxes shown as c' & d') denoted by arrowheads when compared to Gβ3-COS (a & b with highlighted boxes shown as a' & d'). Immunostaining of mTOR and $p70^{S6K}$ revealed co-localisation with CTB-FITC both in untreated (g' & k') and EGF stimulated (h' & l') in Gβ3s-COS while only in EGF stimulated states in Gβ3-COS cells (compare e' and i' with f & j). Images were taken from different fields of view under a 40x objective with further 1.5x magnification. Bar = 13µm, bar in highlighted box=3µm.

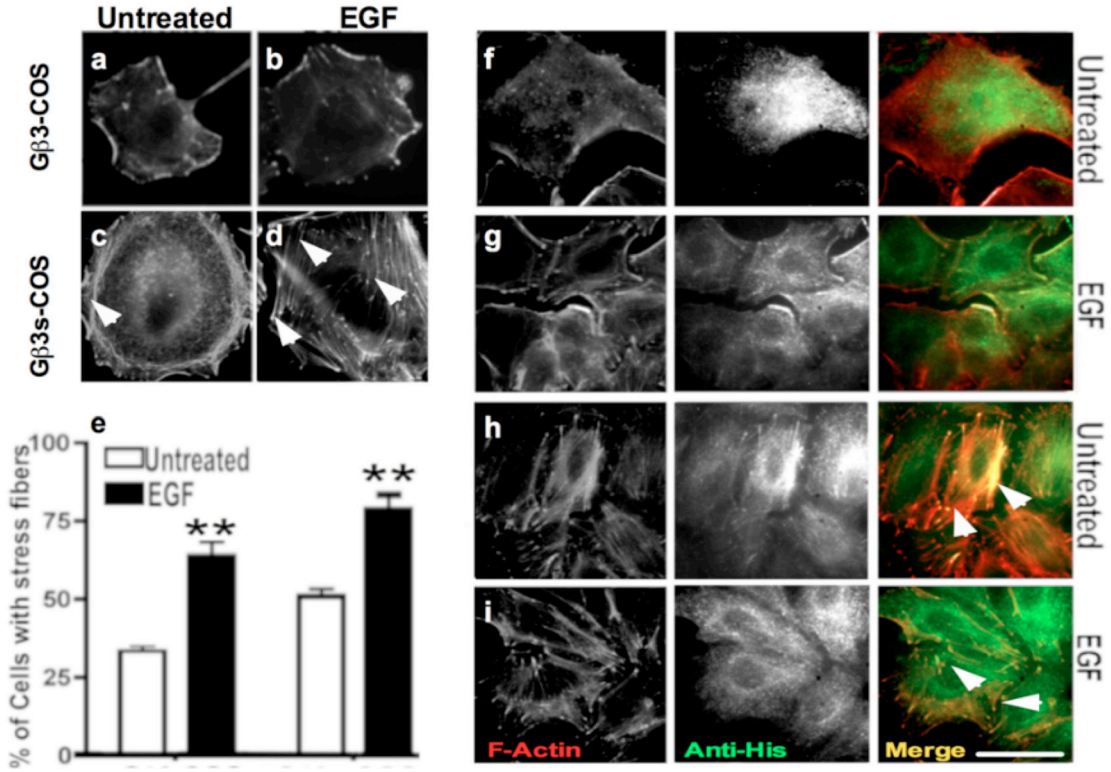

Figure 6. Gβ3s subunit co-localises with F-actin and enhances actin stress fiber formation. Gβ3-COS and Gβ3s-COS cells were either left untreated or treated with EGF followed by F-actin staining using Alexa fluor 568 conjugated phalloidin. Gβ3s-COS cells exhibit enhanced stress fiber formation (white arrow heads) both in untreated (c) and EGF stimulated (d) when compared to Gβ3-COS untreated (a) and EGF stimulated (b). The number of cells exhibiting stress fiber formation were counted as mentioned in material and methods and plotted as graph to represent % of stress fiber forming Gβ3s-COS and Gβ3-COS cells (e). Increased Anti-His staining and co-localisation within F-actin stress fibers (arrow heads) is observed in HA-Gβ3s-COS cells both in basal (h) and EGF treated states (i) when compared to anti His staining of HA-Gβ3-COS (f, g). Images were taken from different fields of view under a 40x objective with further 1.5x magnification. Bar = 13μm.

Presence of Gβ3s variant enhances cell migration and scratch wound healing

A number of findings made in our investigation uncovered signaling alteration specific to the presence of Gβ3s not only in PI3K and MAPK pathway substrates, but also in second messengers and overall cytoskeletal remodeling. Cav-1 expression and phosphorylation is known to be associated with enhanced cell migration especially in fibroblasts, where caveolin-1 expression and phosphorylation at Y-14 residue are proven to be essential to promote migration [49]. Moreover activation of $p70^{S6K}$ leads to expression and proteolytic activity of matrix metalloproteinase (MMP)-9 and cellular invasion in ovarian cancer cells [50]. Finally, we found greater nuclear retention of Foxo3a, which was previously found to induce MMP-9 and MMP-13 expression resulting in increased cancer cell invasion [51]. Therefore, enhanced Ca^{+2} influx coupled with ERK hyperphosphorylation following growth factor stimulation, with overall increase in nuclear Foxo3a abundance, Cav1 phosphorylation and formation of actin stress fibers prompted us to investigate whether Gβ3s specific signaling profile would lead to enhanced cell migration.

To answer this, we studied cell migration by performing boyden chamber based migration assays using different migratory and Ca^{2+} stimulating ligands on Gβ3s/Gβ3 expressing TT lymphoblastoids and only Gβ3 expressing CC lymphoblastoid cells. We found that TT lymphoblastoid cells under control (BSA stimulated) conditions had a significantly larger number of migrating cells than CC cells (figure 8a). Moreover, following ligand stimulation by EGF, Vascular Endothelial Growth Factor (VEGF) and Transforming Growth Factor α (TGFα), the number of migrating cells increased for both CC and TT cell types (figure 8a). However, upon ligand stimulation, the latter cell type showed a significantly greater number of migratory cells than the former, especially for EGF treatment, which led to almost twice the number of motile TT cells as compared to CC (figure 8a). The migratory difference following EGF stimulation is also displayed as a % change from the basal rate, normalized to 100% for both CC and TT cell types (figure 8b). According to this figure, following stimulation with ligand, the % of migrated cells doubled in TT cells, as compared to CC cells where only a modest increase was observed.

In a similar experiment, scratch wound healing assays

on stable COS7 clones of Gβ3 and Gβ3s was performed. Scratch wound healing assay revealed enhanced kinetics of wound healing of Gβ3s-COS cells (figure 8f & g) as compared to Gβ3-COS cells (figure 8d & e) 24hrs post scratch and stimulation with EGF. The enhanced surface area covered by Gβ3s-COS when compared to Gβ3-COS post scratching reveals that Gβ3s subunit expression (figure 8f) induced enhanced migration kinetics, but not cell proliferation (figure 1a & b).

Taken together, these findings suggest that lower comparative activation of AKT1, but enhanced mTOR and downstream substrate phosphorylation suggest that a second regulatory pathway responds to growth factor stimulation only in the presence of the Gβ3s subunit to promote enhanced migration.

Gβ3s-induced cell migration is dependent upon Ca^{2+} influx-regulated ERK but independent of AKT1 and mTOR

Gβγ effector signalling is primarily regulated through Ca^{+2} ion flux, which in turn activates various signaling pathways that control cell migration [6]. Gβγ stimulates Ca^{2+} ion influx from the extracellular space, leading to the activation of calmodulin and inactivation of the IP3 receptor. In order to dissect and identify the signaling pathways regulated by Gβ3s subunit in inducing enhanced cell migration as shown here, we individually targeted different components of pathways downstream of Gβγ signaling and studied its effect on phosphorylational induction of key substrates, dynamic changes in Ca^{2+} ion fluxes and their consequences for cell migration and scratch wound healing.

First of all, in order to characterize the role of Ca^{2+} ion flux in Gβ3s induced migration, we blocked the calcium channels using verapamil, an L-type calcium channel blocker. We saw inhibition of EGF stimulated intracellular Ca^{2+} ion influx following verapamil treatment in both TT and CC cells. However, this inhibition was to a lesser extent in TT lymphoblasts as compared to the CC counterparts (figure 9a). Interestingly, verapamil treatment led to increased AKT1 phosphorylation at both T-308 and S-473 residues in CC and TT cells (figure 10a & c) as

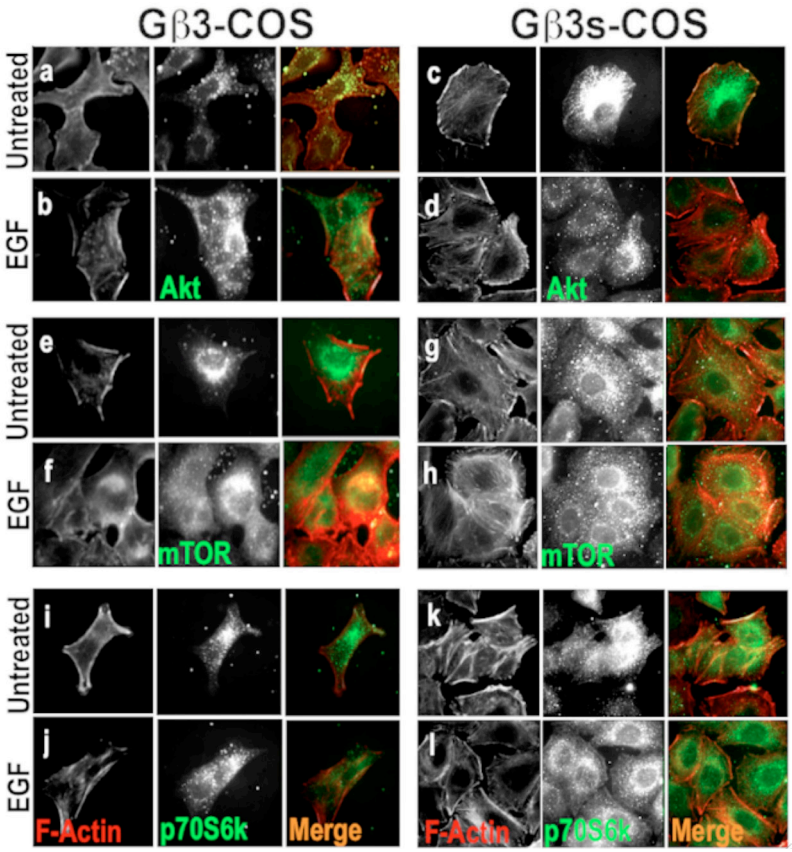

Figure 7. Gβ3s subunit displaces AKT away from actin stress fibers. F-actin staining using Alexa fluor 568 conjugated phalloidin and co-immuno staining using antibodies against total AKT1, mTOR and $p70^{S6k}$ and subsequent relevant secondary antibody conjugated to alexafluor-488 was performed for both Gβ3-COS and Gβ3s-COS cells (a-i). While Gβ3-COS exhibit co-localisation between F-actin and AKT1, Gβ3s-COS cells fail to show such co-localisation both in untreated and EGF treated states (compare a & b with c & d). Gβ3s-COS cells exhibit enhanced co-localisation of mTOR and $p70^{S6K}$ with F-Actin stress fibers as compared to Gβ3-COS cells (compare g, h, k & l with e, f I & j respectively). Images are representative of several images taken from different fields of view under 40x objective with further 1.5x magnification. Bar = 13μm. Data are the mean with standard error (bars) of n=3 independent experiments (n). Statistical significance is shown as *P<0.05, **P<0.01, ***P<0.001.

compared to untreated cells (figure 3b). As expected, this AKT1 activation also led to a corresponding increase in Foxo3a phosphorylation in EGF stimulated cells following Verapamil treatment (figure 11a). To confirm the role of Ca^{2+} ion influx in regulating ERK activation, we blotted for total and phospho ERK and found that upon Ca^{2+} influx inhibition, phospho ERK levels dropped and the degree of reduction of ERK activity corresponded well with the degree of Ca^{2+} ion inhibition achieved with verapamil in the CC and TT cell line models (10 a & b). This confirmed the earlier assumption that EGF stimulated ERK induction is as a result of enhanced cytosolic Ca^{2+} ion influx in Gβ3s containing cells. Moreover, while the phosphorylated levels of mTOR and 4E-BP1 showed a decrease upon inhibition of Ca^{2+} influx (figure 11c & e), there was an overall increase in $p70^{S6K}$ T-389 phosphorylation (figure 11d) in TT cells as compared to the CC counterparts.

In Rat-1 fibroblasts, phosphorylation of 4E-BP1 was shown to occur via a pathway that was Ca^{2+} and calmodulin dependent [52]. Intracellular Ca^{2+} ions were also shown to induce $p70^{S6k}$ phosphorylation upon ionomycin or thapsigargin treatment independent of AKT1in Balb/c-3T3 fibroblasts [53]. Since there was a decrease in Ca^{2+} influx following verapamil treatment in EGF stimulated cells (figure 9a), the increase in $p70^{S6k}$ phosphorylation (figure 11d) following this treatment in Gβ3s cells could be independent of Ca^{2+}. As there was AKT1 activation, this upregulation of $p70^{S6k}$ phosphorylation could have resulted from AKT1. Overall, we found that inhibition of Ca^{2+} influx reduced ERK, mTOR and 4E-BP1, but increased ATK1 and $p70^{S6k}$ phosphorylation.

We next studied the effects of MEK inhibition on these signaling components. Targeting MEK in the Ras/Raf/MEK/ERK pathway is advantageous as it is a convergence

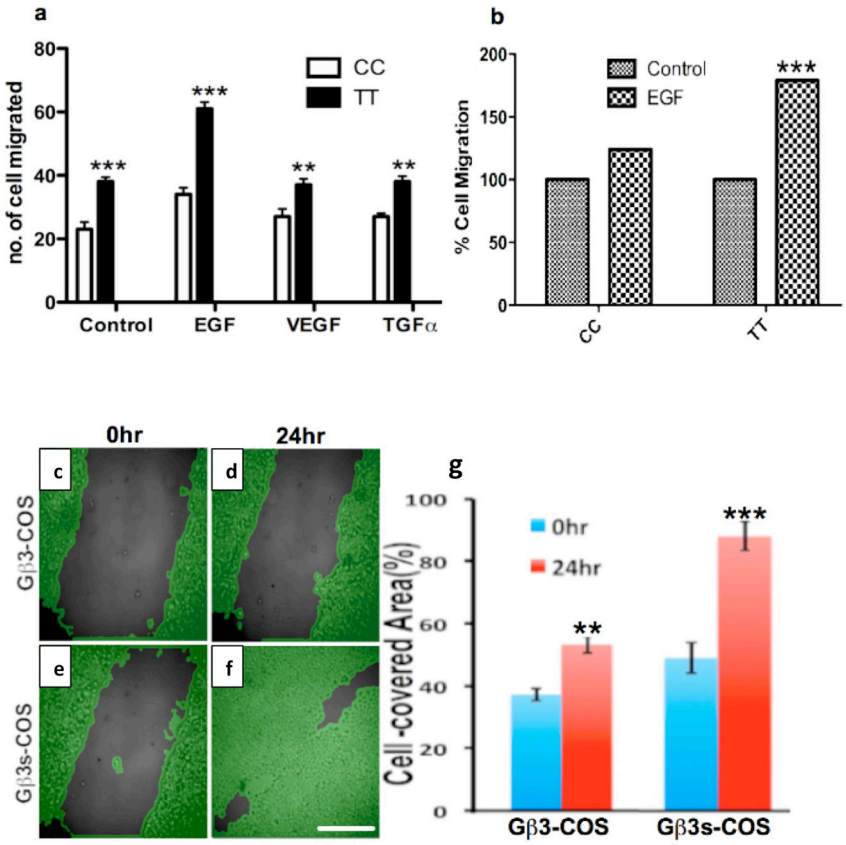

Figure 8. The presence of Gβ3s subunit enhances cell migration. CC and TT lymphoblastoids were either left untreated, or treated with growth factors and subjected to boyden chamber based chemotactic migration assay to examine their relative differences in migration. EGF, TGFα and VEGF stimulated enhanced chemotactic migration of serum starved TT lymphoblast cells as compared to CC (a). Control refers to 5% BSA stimulation in both CC and TT lymphoblast cells. The percentage of cell migration upon EGF stimulation is high in TT when compared to CC (b). Data presented in all panels are the mean with standard error (bars) of n = 3 independent experiments performed in octuplets. Statistical significance is shown as * P<0.05, **P<0.01, ***P<0.001. For scratch wound assays (c-g), scratches were made with a fine tip on coverslips containing stable clonal adherent Gβ3 and Gβ3s COS-7 cell lines. COS-7 stable clone expressing Gβ3s subunit showed greater gap closure 24hr post scratching (c & d) when compared to COS-7 stable clones expressing normal Gβ3 subunit (e & f). Graphical representation of % area covered by cells following 24hr of wound healing (h). These images are taken from different fields of view under a 5x objective with further 1.5x magnification. Bar = 100μm. WIMASIS analysis tool was used to measure area covered by cells as mentioned in the methods section (e). Data presented in all panels are the mean with the standard error (bars) of n = 3 independent experiments. Statistical significance is shown as *P<0.05, **P<0.01, ***P<0.001.

point for upstream signaling pathways controlled by AKT and ERK. ERK is known to be activated by MEK in a calcium sensitive pathway also involving modulation by cAMP via PKA. We found maximum inhibition of EGF induced cytosolic Ca^{2+} influx upon treatment with U0216, a MEK inhibitor (figure 9c). This correlates well with inhibition of ERK phosphorylation as expected (figure 10a).

Treatment of U0216 resulted in modest induction of AKT phosphorylation at both T-308 and S-473 residues in CC and TT lymphoblasts (figure 10a & d) when compared to untreated cells (figure 3b). A significant decrease in phospho 4E-BP1 threonine-46 residue was observed (figure 11a & e) upon MEK inhibition even though there was activation of mTOR and $p70^{S6K}$ (figure 11a, c & d). This suggests that the mTOR pathway activation via MEK inhibition might not involve a protein translation function. Previous studies reported the participation of Raf-1/MEK/ERK in crosstalk with 4E-BP1, leading to increased protein synthesis, cell growth, and kidney tumor formation (54). The drop in 4E-BP1 phosphorylation observed here or alternatively its activation (figure 3b) corresponded well with ERK activity rather than mTOR>$p70^{S6k}$ activation in both CC and TT lymphoblast cells (figures 10 & 11).

Next, in order to directly target upstream signaling emerging from G proteins, we used a GRK2 polypeptide (GRK2i), which acts as a cellular Gβγ antagonist by inhibiting binding to Gβγ dimer and sequester its signaling activity [55]. Following GRK2i treatment of both CC and TT lymphoblastoids, there was a modest decrease of EGF stimulated cytosolic Ca^{+2} ion influx in TT cells and complete inhibition in CC counterparts (figure 9b). GRK2i treatment also caused a significant decrease in ERK phosphorylation CC lymphoblastoids, while to a lesser extend in the Gβ3s containing TT counterparts (figure 10a & b). Moreover, while phospho AKT at S-473 was inhibited, AKT phosphorylation at T-308 (figure 10a & c) and mTOR S-2481 (figure 11a & c) were still maintained. Only partial inhibition of ERK phosphorylation in GRK2i treated Gβ3s containing cells as compared to their Gβ3 counterparts could be based on the fact that following this treatment, there was still sufficient cytosolic calcium influx upon EGF treatment in TT cells as compared to CC where a complete inhibition was seen (figure 9b).

We finally studied the effects of the above treatments on cell migration of TT and CC cells, kinetics of scratch wound healing in Gβ3-COS and Gβ3s-COS cells and actin stress fiber formation. We found that inhibition of cytosolic Ca^{2+} influx following verapamil treatment inhibited EGF induced migration of TT lymphoblast cells down to their untreated levels (figure 12a). This implied the involvement of Ca^{2+} dependent activation of ERK in the enhanced migration of Gβ3s cells as well as an AKT independent phenomenon. This further suggests that Gβγ signaling induces hyper Ca^{2+} influx, which primarily contributes to the activation of ERK and mTOR activity, leading to enhanced migration only in the presence of a Gβ3s subunit but not in its absence. In a similar experiment, we found that the kinetics of wound healing in Gβ3s-COS were also significantly reduced upon verapamil treatment (compare figure 2e & f with figure 13g & h) also probably explaining the absence of EGF induced actin stress fiber formation following such treatments (compare figures 6d & 13x).

Hence, the elevation of AKT T-308 residue phosphorylation upon Verapamil treatment was not sufficient to potentiate migration kinetics in both the CC and TT lymphoblast cells (figure 12a) and COS7 stable clones (figure 13 a, b & g, h & 12 m, n). This implied that at signal effector level, the involvement of ERK was critical for the enhanced Gβ3s migration. Indeed, when the MEK inhibitor, U0216 was employed, which

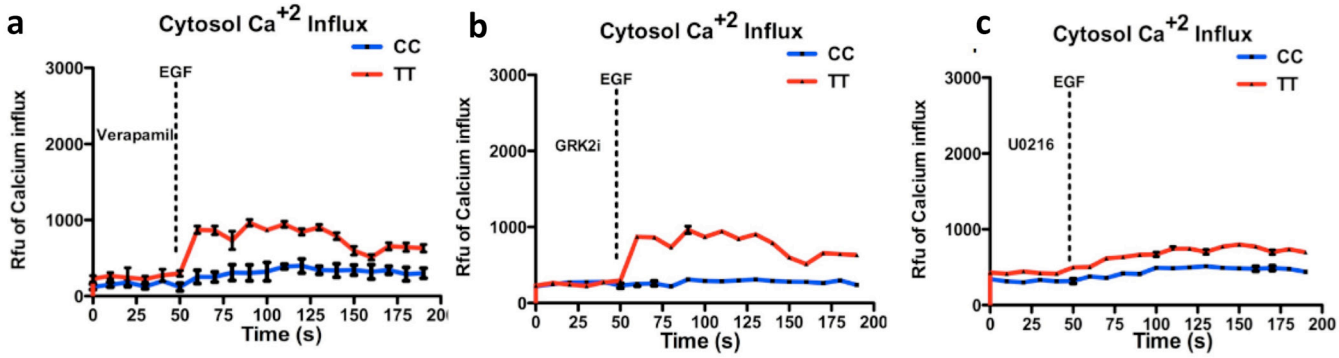

Figure 9. Cytosolic Ca^{2+} influx in Gβ3s containing cells responds differently to growth signaling inhibitors. CC and TT cells were exposed to a co-treatment of Gβγ signaling inhibitors and EGF and in parallel, temporal changes in intracellular cytosolic Ca^{2+} influx were quantified by employing Fluo-4 NW based Ca^{2+} assay as mentioned in materials and methods. Treatments with calcium ion channel blocker Verapamil, Gβγ signaling inhibitor GRK2i, and MEK inhibitor U0216 caused decrease in EGF induced cytosolic Ca^{2+} levels (a, b and c respectively) in both TT and CC lymphoblast cells, however, EGF induced Ca^{2+} levels in TT lymphoblasts were more resistant to inhibitors than the CC counterparts. Inhibition of MAPK pathway by way of using MEK inhibitor U0216 was found to be most potent in inhibiting cytosolic Ca^{2+} ions in TT lymphoblast cells. Data presented in all panels are the mean with a standard error (bars) of n = 3 independent experiments performed in octuplets. Statistical significance is shown as *P<0.05, **P<0.01, ***P<0.001.

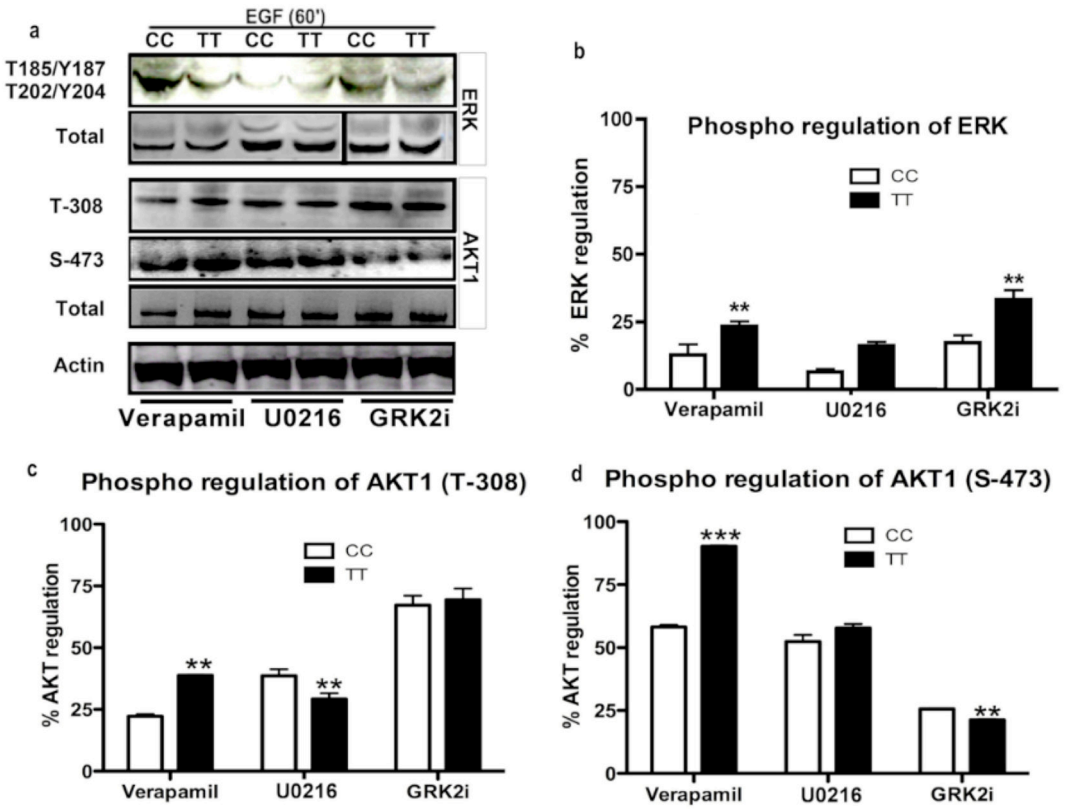

Figure 10. The presence of Gβ3s causes altered ERK and AKT signaling response to growth inhibitory treatments: TT and CC lymphoblasts were exposed individually to calcium ion channel blocker Verapamil, Gβγ signaling inhibitor GRK2i, and MEK inhibitor U0216 to study the effects of such treatments on their EGF induced phospho ERK and AKT1 signaling profiles. While EGF induced ERK phosphorylation was disrupted in TT lymphoblasts following treatments with any of the inhibitors with most inhibition achieved following MEK inhibition (a & b), phospho AKT1 Serine 473 levels were found to be enhanced upon verapamil treatment in TT cells as compared to CC counterparts (d). Distinct responses to inhibitor treatments as exhibited by TT and CC lymphoblasts are confirmed by semi quantitative densitometry analyses. Data presented in all panels are the mean with standard error (bars) of n = 3 independent experiments. Statistical significance is shown as *P<0.05, **P<0.01, ***P<0.001.

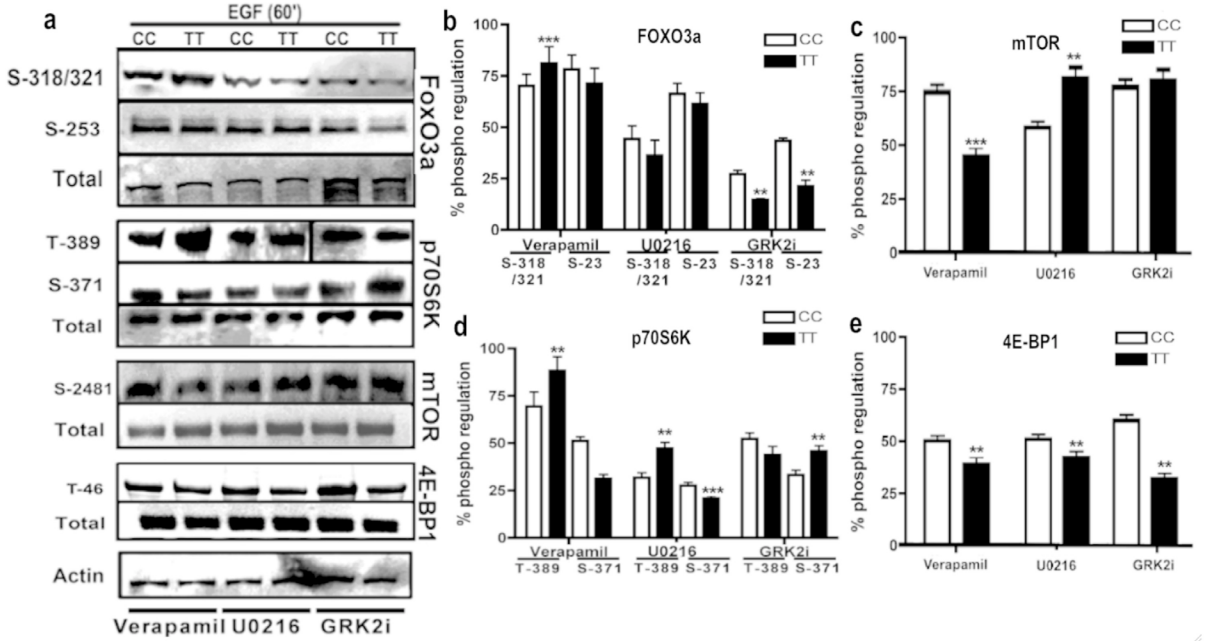

Figure 11. Inhibition of EGF-induced mTOR, 4E-BP1, p70^{S6K} and Foxo3a signalling in TT and CC lymphoblasts exhibit distinct responses. Phospho immunoreactivity of mTOR, 4E-BP1, p70S^{6K} and Foxo3a upon treatment with Gβγ signaling inhibitors shows altered signaling response in TT cells in comparison to CC lymphoblasts. The distinct signaling profiles are confirmed by semi quantitative densitometry analyses. Data presented in all panels are the mean with standard error (bars) of n = 3 independent experiments. Statistical significance is shown as *P<0.05, **P<0.01, ***P<0.001.

as expected, inhibited phospho ERK levels, not only abrogated cytosolic Ca^{2+} levels (figure 9c), but also resulted in complete inhibition of enhanced cell migration of TT cells (figure 12c), closer to 0% closure of the scratched surface after 24hr of healing time (figure 13i & j) and absence of any stress fiber formation (figure 13y). Treatment with GRK2i could not completely inhibit the EGF induced enhanced migration of Gβ3s cells (figure 12b) and there was some degree of scratch wound healing (figure 13 k & l). Failure of GRK2 inhibition to exert complete disruption of migration could be because it could not completely prevent EGF induced Ca^{2+} influx (figure 9b), or phospho ERK induction (figure 10b).

Altogether, these results indicate hyperactivation of a signaling pathway that is unique to the presence Gβ3s, which provide for a mechanism of enhanced migratory phenotype exhibited only by cells containing the Gβ3s variant and not normal Gβ3 protein. According to this mechanism, EGF stimulation leads to induction of supranormal levels of cytosolic Ca^{2+} that activate and cross-talk with MAPK pathway resulting in hyperphosphorylated ERK. The low levels of cAMP and phospho AKT in Gβ3s containing cells also result in activation of Foxo3a transcription factor and phosphorylation of Cav1 caveolae protein that contribute in cytoskeletal remodeling, formation of actin stress fibers and enhanced migration upon growth factor stimulation.

Gβ3s subunit signaling leads to Rho, Rac, and cdc-42 GTPases activation

Members of the Rho family of small guanosine triphosphatases have emerged as key regulators of the actin cytoskeleton, through their interaction with multiple target proteins [56]. Moreover, Ca^{2+} influx plays a major role in RhoA activation and in linkage of the RhoA/stress fiber cascade to the focal adhesion kinase pathway [57]. Rac activation was previously reported to involve Cav1 Y-14 phosphorylation in mouse melanoma cells [49] while Cav1 phosphorylation was also demonstrated to influence RhoA, RhoB and RhoC and its downstream effector, ROCK in order to promote cell migration and invasion [58]. Similarly, Rac2 and CDC42 were found to be required for actin assembly to drive cellular translocation [58] while inhibition of ROCK reduced metastasis *in vivo* [59]. Thus the cytoskeletal remodeling involving actin stress fiber formation, Cav1 phosphorylation and the enhanced migration observed in Gβ3s containing cells led us to investigate if the Rho, Rac and CDC-42 GTPases regulation is also altered because of the presence of Gβ3s subunit.

To our surprise, in Gβ3s subunit expressing TT lymphoblasts, we observed enhanced Rho A expression and also increase in phosphorylation activity of RhoA and Rac1-2-3/CDC-42 at S-71/73 respectively (figure 14a). TT lymphoblast cells showed decreased expression of Rho A when treated with verapamil in comparison to treatments with other inhibitor (figure 14b). Hence, Rho A expression showed correlation with cytosolic Ca^{2+} ions (figure 2). The enhanced RhoA expression and activity in Gβ3s-COS cells appeared to localise in actin stress fibers at both basal and EGF stimulated conditions (figure 14g, i & m & o) in comparison to the RhoA expression in Gβ3-COS cells (figure 14d, f & j & l).

Discussion

This study reports interesting findings of Gβ3s subunit signaling in regulating and stimulating distinct molecular

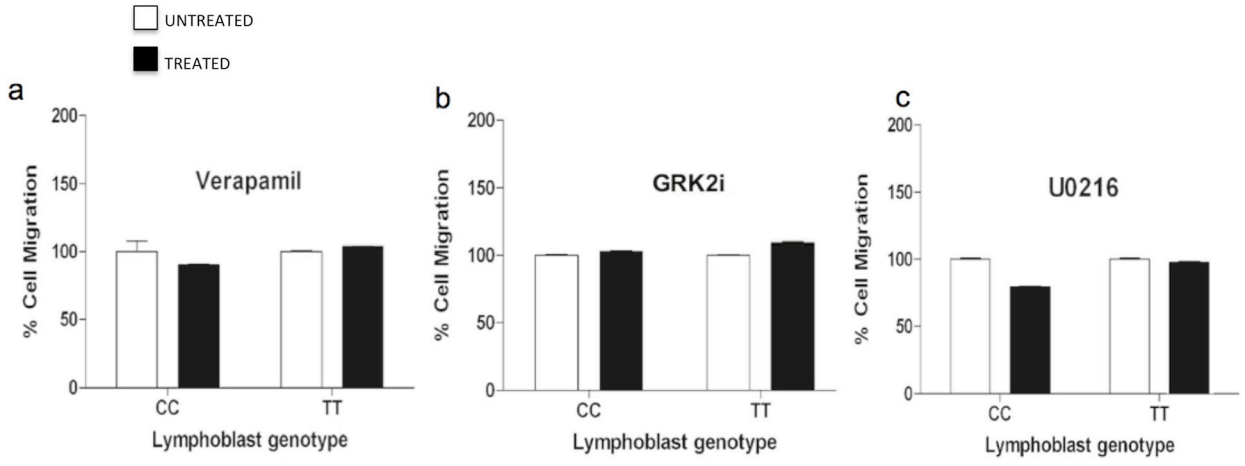

Figure 12. Gβ3s-induced enhance cell migration is blocked by ERK or Ca^{2+} ion channel inhibition confirming that Gβ3s associated migration is a Ca^{2+} regulated phenomenon. Boyden chamber assay on serum starved CC and TT lymphoblast cells was performed to study the effect of Gβγ signaling inhibitors on EGF stimulated chemotactic migration. Control is represented as 100% migration and refers to 5% BSA stimulation in both CC and TT lymphoblast cells. While ERK and Ca^{2+} ion channel inhibition caused complete disruption of EGF-stimulated enhanced migration of TT cells, GRK2i inhibition only caused partial inhibition of growth factor induced migration. Data presented in all panels are the mean with standard error (bars) of n = 3 independent experiments performed in octuplets. Statistical significance is shown as *P<0.05, **P<0.01, ***P<0.001.

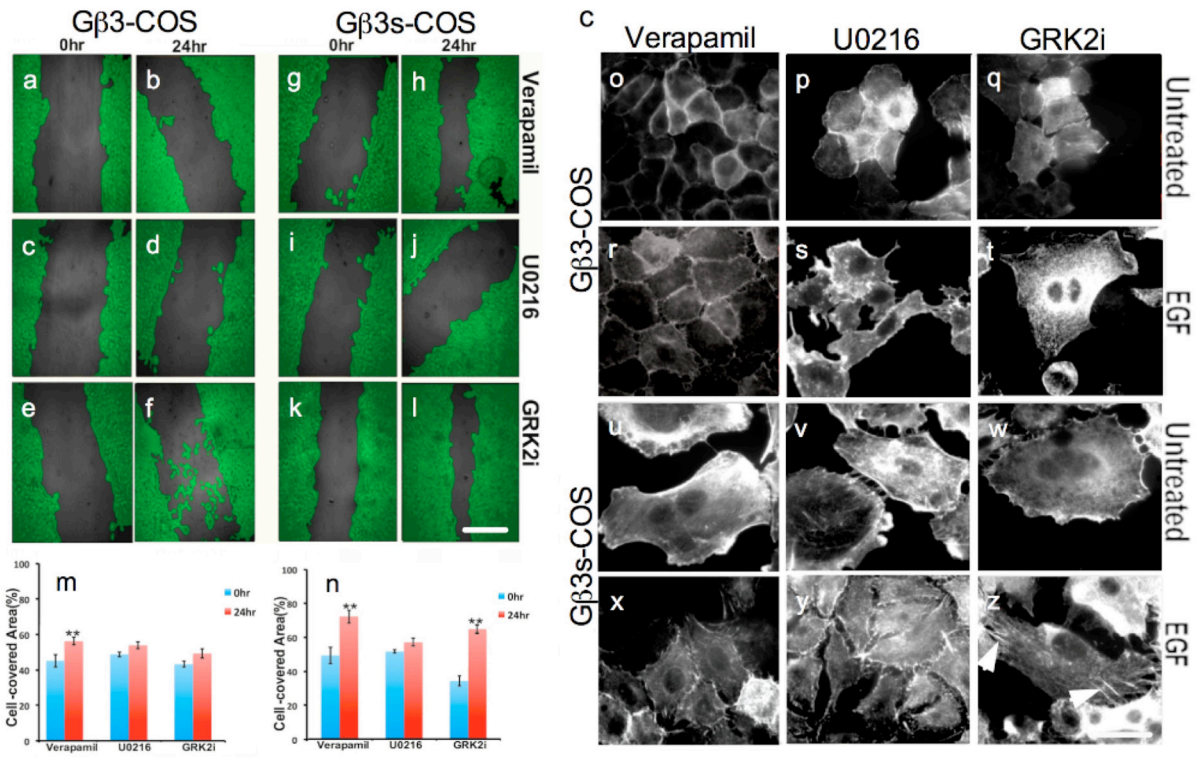

Figure 13. Disruption of Actin stress fiber formation inhibits cell migration. The degree of wound gap closure was studied in Gβ3-COS and Gβ3s-COS cells by scratch wound assay (c-l) for which, scratches were made with a fine tip on coverslips containing stable clonal adherent Gβ3 and Gβ3s-COS cell lines. Scratch wound healing assay revealed greater decrease in gap closure following verapamil (g & h) and U0216 (i & j) treatment while to a lesser extent, following GRK2i treatment (k & l) in Gβ3s-COS cell line. Gap closure in Gβ3-COS cell was sensitive to all inhibitor treatments (a-f). This indicated the involvement of Ca^{+2} ions and ERK pathway in the enhanced scratch wound healing kinetics of Gβ3s-COS cell line. Images are taken from different fields of view under a 5x objective with further 1.5x magnification. Bar = 100μm. Graphical representation of the cell covered area as analyzed by WIMASIS tool as mentioned in materials and methods section (m-n). Data presented in all panels are the mean with standard error (bars) of n = 3 independent experiments. Statistical significance is shown as *P<0.05, **P<0.01, ***P<0.001. Actin stress fiber formation was inhibited following Gβγ signaling inhibition indicating the involvement of stress fiber formation for enhanced cell migration of Gβ3s cells. While inhibitor treatments caused total disruption of EGF induced stress fibers in Gβ3-COS cells (o-t), Gβ3s-COS cells still retained some actin stress fibers following GRK2i treatment (indicated arrow heads) (z) indicating only partial inhibition of migration. The images are taken from different fields of view under 40x objective with further 1.5x magnification. Bar = 13μm.

dynamics affecting AKT and ERK activation. This occurs through the induction of cytosolic Ca^{2+} influx activating ERK, mTOR and $p70^{S6K}$ leading to reorganisation of actin cytoskeleton to enhance cell migration.

We observed hyper induction of cytosolic Ca^{2+} ions in response to EGF stimulation only in Gβ3s subunit expressing cells (figure 2). The rise in cytosolic calcium is likely to activate classical isoforms of protein kinase C (PKC), which moves from the cytosol to the membrane, where it is further activated by DAG [60]. In aortic endothelial cells, during arteriogenesis of mice and zebrafish, suppression of the PI3K/AKT signaling pathway resulted in an increased activation of ERK1/2 [61]. This suggests that the activation of ERK1/2 in the TT lymphoblasts may be a compensatory mechanism for the loss of PI3K/AKT pathway activity. Ca^{2+} influx plays a crucial role as key mediator of intracellular signaling regulated by the Gβγ pathways, which in turn control various biochemical events. Hyper regulation of calcium has previously been shown to increase the rate of PLCβ enzyme catalysis, which in turn leads to the production of IP3. In H9c2 cells, overexpression of calreticulin triggered calcium influx that reduced AKT activation via protein phosphates 2A and increased cell susceptibility to apoptosis [62]. Long-term elevation of calcium stimulated through thapsigargin in H9c2 cells were also reported to suppress AKT activity while long term reduction of calcium recovered AKT activity [63]. While it is now known that ERK is primarily activated by growth factors such as EGF by either Ras-dependent or Ras-independent pathways leading to activation of the Raf/MEK/ERK cascade, how EGF affects gene expression that alters cell migration and motility remains largely unknown. One study reported that EGF stimulation of fibroblast motility is dependent on hyaluronan synthesis [64].

G proteins regulate AKT1 by two distinct and potentially opposing mechanisms. These are by activation through Gβγ dimers in a PI3k dependent fashion and

inhibition mediated by Gαq. Hence AKT1 is considered as a novel point of convergence between disparate signaling pathways. AKT1 serves as a multifaceted intermediary signaling to the diversified downstream biological effectors and as such has received much attention for the versatile roles it plays in various biological processes. Therefore the activation of AKT substrates such as mTOR (figure 3b) in the absence of AKT activation itself is a consequence of cross talk probably due to high ERK phosphorylation (figure 3a) resulting from the signaling unique to the presence of the Gβ3s subunit. Reduction of AKT1 T-308 phosphorylation in TT lymphoblast cells (figure 3a) might suggest that in the presence of Gβ3s, the targets of AKT1 phosphorylation (T-308) such as GSK3α/β, Foxo transcription factors, Bad, $p21^{Cip1}$, and $p27^{Kip1}$ will be affected. Enhanced phosphorylation of mTOR, $p70^{S6K}$ and ERK in the absence of AKT1 activation in TT lymphoblast cells suggests that the effectors of AKT1 might be redirected for control through ERK to compensate for the lack of AKT1 signaling. Phosphorylation of PI3K results in the conversion of PIP2 to PIP3. PIP3-triggered translocation of AKT1 from the cytoplasm to the plasma membrane is a prerequisite for its phosphorylation and activation [65]. In addition to altered phosphorylation of AKT1, we also saw distinct translocation kinetics of AKT1 in Gβ3s-COS cells (figure 5 & 7).

Recent studies have also shown that the AKT2 isoform is an enhancer of cell migration and invasion *in vitro* and *in vivo*, and the related AKT1 isoform may function as an inhibitor of these metastatic phenotypes [66-68]. Moreover it has been identified that treatment with Migration Stimulating Factor (MSF), a truncated form of fibronectin promotes the migration in human fibroblasts and endothelial cells, upon inhibiting AKT activity [69]. Thus, downregulation of AKT1 phosphorylation through Gβ3s signaling seems to be important for the enhanced migratory phenotype.

The observed signaling alterations unique to the presence of *Gβ3s* could exhibit a distinctive translational control. Firstly, Foxo3a is a key regulator of ubiquitin mediated proteolysis [70], which suggests that there is an increased rate of protein breakdown in TT lymphoblasts owing to increased Foxo3a stability (reduced phosphoFoxo3a) as compared to CC counterparts (figure 3b & c). This would lead to higher turn over of proteins and increase in amino acid availability. Calcium inhibition upon verapamil treatment, on the other hand, resulted in reduction of EGF mediated Foxo3a stability (increased phosphorylation) in TT cells (figure 11a & b). Therefore Foxo3a stability appeared to be regulated by cytosolic calcium ions perhaps through its effects on

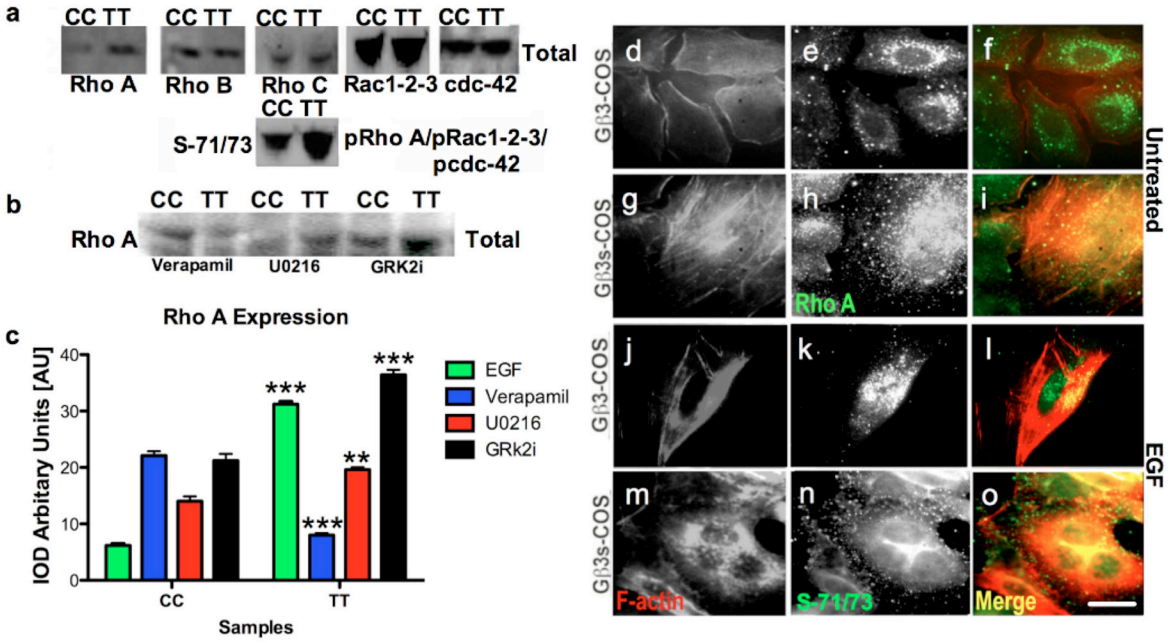

Figure 14. Contribution of RhoA in Gβ3s subunit specific cell migration phenotype. Immuno reactivity of total RhoA, RhoB, RhoC, Rac 1-2-3 and CDC42 and phospho immuno reactivity of Rho A at S-73 and Rac 1-2-3, cdc42 at S-71 upon EGF stimulation were determined by western blotting. TT lymphoblast lysates showed enhanced total RhoA expression and RhoA/Rac 1-2-3/cdc-42 activity when compared to normal CC (a). Rho A expression was analysed in CC and TT lymphoblast cell lysates upon stimulation with EGF in the presence of inhibitors (b). Data presented in all panels are the mean with standard error (bars) of n = 3 independent experiments. Statistical significance is shown as *P<0.05, **P<0.01, ***P<0.001. Gβ3s-COS cells showed enhanced co-localisation of RhoA (g-i) and phosphorylated RhoA, Rac 1-2-3 and CDC42 (m-o) with actin stress fibers. The images are taken from different fields of view under 40x objective with further 1.5x magnification. Bar = 13μm.

AKT1 phosphorylation. Secondly, in our study we found that *Gβ3s* cells exhibited increased phospho 4E-BP1 while inhibition of the elevated Ca^{+2} ions in *Gβ3s* cells led to inhibition of phospho4E-BP1. In hippocampal neurons, ERK1/2 has been shown to control 4EBP-1 phosphorylation [71]. We found that inhibition of the hyperphosphorylated ERK1/2 following MEK inhibition resulted in a similar reduction of phospho 4E-BP1 levels as well. Thirdly, amino acid availability due to increased protein breakdown will also result in mTOR activation as mTOR has been shown to be directly activated by intracellular amino acid concentration [72, 73]. Consistent with this, we found 2-fold increase in mTOR phosphorylation in TT cells as compared to CC cells. Finally, we also found increased $p70^{S6K}$ phosphorylation in TT cells (figure 3b).

In adult cardiomyocytes, tissue plasminogen activator was shown to activate $p70^{S6K}$ in a non-AKT dependent manner through c-Raf/ERK1/2 pathway [74]. ERK1/2 was also found to form a complex with $p70^{S6K}$, suggesting ERK1/2 to be the main kinase for $p70^{S6K}$ phosphorylation at one or more amino acid residues [75], while phosphorylated $p70^{S6K}$ is known to primarily control actin cytoskeleton dynamics through involvement of F-actin micro domain signaling, stress fiber disruption and directional migration of cells [76, 77]. These examples indicate a cross-talk mechanism operating between mTOR and ERK1/2 pathways in TT lymphoblast cells leading up to activation of downstream targets $p70^{S6K}$ and 4E-BP1 in TT lymphoblast cells (figure 3b). This suggests increased translational activity in TT lymphoblast cells compared to CC lymphoblast cells as well as indicates a stimulated migratory phenotype that we later confirmed in our study. Taken together, these results suggest that Gβ3s presence stimulates altered protein translation in calcium dependent manner involving ERK and mTOR cross talk.

Interestingly, previous reports have shown that Gβγ signaling regulates Ca^{2+} fluxes and the exchange protein activator of cAMP (Epac) to induce cell migration in melanoma cell lines [6]. In Endothelial cells, matrix-specific down-regulation of cAMP/PKA signaling appears to be required for collagen-induced F-actin synthesis and stress fiber formation [76]. cAMP also inhibits the migration of mouse embryonic fibroblasts and 4T1 breast tumor cells by interfering with the formation of lamellipodia at the leading edge during cell migration.

Y-14 phosphorylation of Cav1 is known to be necessary for binding of Cav1 to intermediate filaments, which in turn is required for anterior polarisation at focal adhesion sites for directional transmigration in cells [78, 79]. Furthermore, phosphorylation of Cav1 is an important mechanism for maintaining caveolin hetero- and homo-oligomers and for scaffolding and recruitment of signaling components to caveolin associated complexes. This results in stabilisation of multiprotein complexes between caveolar resident and cytoskeletal proteins to regulate cell signaling [80]. Vascular endothelial growth factor has been shown to trigger src dependent Cav1 phosphorylation that resulted in induction of migration in myeloma cells. Moreover, Gβγ signaling induces Src kinase activation to activate caveolae by establishment of cell polarity [39]. Previous studies have shown that upon disruption of cytoskeleton using inhibitors (e.g.: cytochalasin D), the levels of cAMP increased, thereby, causing aberration in signal transduction (81). We found induction of phospho Cav1 (figure 4a) to reorganise actin filament structure and enhance stress fibers (figure 5 & 6) through downregulation of cAMP (figure 4b). Hence, the induction of Cav1 phosphorylation and establishment of actin stress fibers in the presence of Gβ3s represents itself as the downstream mechanism of altered signaling leading to enhanced migration.

Gβ3s is primarily implicated in predisposition to hypertension and various cardiac diseases [9]. Importantly, previous studies in hypertensive rat models have demonstrated that a common point in downstream signaling after Ca^{2+} sensitisation and a critical component of hypertension is activation of RhoA and subsequent activation of Rho-kinase [82]. Therefore, the discovery that Gβ3s induced hyper Ca^{2+} influx that led to enhanced expression and activation of RhoA significantly contributes towards our understanding of the increased cancer relapse in certain tumors and hypertension pathology where enhanced kinetics of migration is a prominent phenomenon. Altogether, the current investigation suggests that the enhanced signaling pattern induced by the Gβ3s subunit could be one of the contributing factors of increased migration and metastasis observed in c.825C>T patients with bladder carcinoma and low grade breast tumours [18, 19]. This provides an opportunity to devise therapeutic strategies that specifically target Gβ3 signaling. This strongly suggests a rationale for developing tools for Gβ3s allele specific inhibition as future therapy in these patients.

Acknowledgements

HT, HSK and NZ would like to acknowledge the support given by the Northwood Charitable Trust. MRI is supported by SORSAS award and work in IRE and SJ laboratory is supported by Tattersall Trust and an anonymous trust.

References

1. Entschladen F, Zänker KS, Powe DG. Heterotrimeric G protein signaling in cancer cells with regard to metastasis formation. *Cell Cycle* 2011; **10**(7): 1086-91.
2. Cabrera-Vera TM, Vanhauwe J, Thomas TO, Medkova M, Preininger A, Mazzoni MR,Hamm HE. Insights into G protein structure, function, and regulation. *Endocr Rev* 2003; **24**(6): 765-81.
3. Guzmán-Hernández ML, Vázquez-Macías A, Carretero-Ortega J, Hernández-García R, García-Regalado A, Hernández-Negrete I et al. Differential inhibitor of Gbetagamma signaling to AKT and ERK derived from phosducin-like protein: effect on sphingosine 1-phosphate-induced endothelial cell migration and in vitro angiogenesis. *J Biol Chem* 2009; **284**(27): 18334-46.
4. Tang X, Sun Z, Runne C, Madsen J, Domann F, Henry M et al. A critical role of Gbetagamma in tumorigenesis and metastasis of breast cancer. *J Biol Chem* 2011; **286**(15): 13244-54.
5. Kirui JK, Xie Y, Wolff DW, Jiang H, Abel PW, Tu Y. Gbetagamma signaling promotes breast cancer cell migration and invasion. *J Pharmacol Exp Ther* 2010; **333**(2): 393-403.
6. Baljinnyam E, Umemura M, De Lorenzo MS, Xie LH, Nowycky M, Iwatsubo M et al. Gβγ subunits inhibit Epac-induced melanoma cell migration. *BMC Cancer* 2011; **11**(256): 1471-2407
7. Castellano E, Downward J. RAS Interaction with PI3K: More Than Just Another Effector Pathway. *Genes Cancer* 2011; **2**(3): 261-74.
8. Altomare DA, Testa JR. Perturbations of the AKT signaling pathway in human cancer. *Oncogene* 2005; **24**(50): 7455-64.
9. Siffert W, Rosskopf D, Siffert G, Busch S, Moritz A, Erbel R., et al. Association of a human G-protein β3 subunit variant with hypertension. *Nat Genet* 1998; **18**(1): 45–48.
10. Tummala H, Ali M, Getty P, Hocking PM, Burt DW, Inglehearn CF, Lester DH. Mutation in the guanine nucleotide-binding protein beta-3 causes retinal degeneration and embryonic mortality in chickens. *Invest Ophthalmol Vis Sci* 2006; **47**(11): 4714-8.
11. Tummala H, Fleming S, Hocking PM, Wehner D, Naseem Z, Ali M, et al. The D153del mutation in GNB3 gene causes tissue specific signalling patterns and an abnormal renal morphology in Rge chickens. *PLoS One* 2011; **6**(8): e21156.
12. Virchow S, Ansorge N, Rosskopf D, Rübben H, Siffert W. The G protein beta3 subunit splice variant Gbeta3-s causes enhanced chemotaxis of human neutrophils in response to interleukin-8. *Naunyn Schmiedebergs Arch Pharmacol* 1999; **360**(1): 27-32.
13. Tummala H, Khalil HS, D Ascanio I, Wehner D, Lester DH, Babraj John et al. Human 825C>T polymorphism in GNB3 gene promotes enhanced cell migration by inducing cytosolic calcium influx and hyper phosphorylation of ERK regulated mTOR pathway. *FEBS J* 2012; **279**(1) p. 141.
14. Goldlust IS, Hermetz KE, Catalano LM, Barfield RT, Cozad R, Wynn G, et al. Mouse model implicates GNB3 duplication in a childhood obesity syndrome. *Proc Natl Acad Sci U S A* 2013; **110**(37): 14990-4.
15. Dobrev D, Wettwer E, Himmel HM, Kortner A, Kuhlisch E, Schüler S, Siffert W,Ravens U. G-Protein beta(3)-subunit 825T allele is associated with enhanced human atrial inward rectifier potassium currents. *Circulation* 2000; **102**(6):692-7
16. Lindemann M, Virchow S, Ramann F, Barsegian V, Kreuzfelder E, Siffert W,Müller N, Grosse-Wilde H. The G protein beta3 subunit 825T allele is a genetic marker for enhanced T cell response. *FEBS Lett* 2001;**495**(1-2):82-6.
17. Siffert W, Rosskopf D, Moritz A, Wieland T, Kaldenberg-Stasch S, Kettler N, Hartung K, Beckmann S, Jakobs KH. Enhanced G protein activation in immortalized lymphoblasts from patients with essential hypertension. *J Clin Invest* 1995;**96**(2):759-66.
18. Weinstein LS, Chen M, Xie T, Liu J. Genetic diseases associated with heterotrimeric G proteins. *Trends Pharmacol Sci* 2006; **27**(5): 5260–266.
19. Eisenhardt A, Siffert W, Rosskopf D, Musch M, Mosters M, Roggenbuck U et al. Association study of the G-protein beta3 subunit C825Tpolymorphism with disease progression in patients with bladder cancer. *World J Urol* 2005; **23**(4): 279-86.
20. Sheu SY, Handke S, Bröcker-Preuss M, Görges R, Frey UH, Ensinger C et al. The C allele of the GNB3 C825T polymorphism of the G protein beta3-subunit is associated with an increased risk for the development of oncocytic thyroid tumours. *J Pathol* 2007; **211**(1): 60-6.
21. Lehnerdt GF, Franz P, Bankfalvi A, Grehl S, Jahnke K, Lang S et al. Association study of the G-protein beta3 subunit C825T polymorphism with disease progression an overall survival in patients with head and neck squamous cell carcinoma. *Cancer Epidemiol Biomarkers Prev* 2008; **17**(11): 3203-7.
22. Clar H, Langsenlehner U, Krippl P, Renner W, Leithner A, Gruber G et al. A polymorphism in the G protein beta3-subunit gene is associated with bone metastasis risk in breast cancer patients. *Breast Cancer Res Treat* 2008; **111**(3): 449-52.
23. Sambrano GR, Chandy G, Choi S, Decamp D, Hsueh R, Lin KM et al. Unravelling the signal-transduction network in B lymphocytes. *Nature* 2002; **420**(6916): 708-10.
24. Sei Y, Ren-Patterson R, Li Z, Tunbridge EM, Egan MF, Kolachana BS et al. Neuregulin1-induced cell migration is impaired in schizophrenia: association with neuregulin1 and catechol-o-methyltransferase gene polymorphisms. *Mol Psychiatry* 2007; **12**(10): 946–957.
25. Sawa A, Wiegand GW, Cooper J, Margolis RL, Sharp AH, Lawler JF Jr et al. Increased apoptosis of Huntington disease lymphoblasts associated with repeat length-dependent mitochondrial depolarization. *Nat Med* 1999; **5**(10): 1194-8.
26. Sawa A, Nagata E, Sutcliffe S, Dulloor P, Cascio MB, Ozeki Y et al. Huntingtin is cleaved by caspases in the cytoplasm and translocated to the nucleus via perinuclear sites in Huntington's disease patient lymphoblasts. *Neurobiol Di* 2005; 20**(2)**: 267-74.
27. Nagata E, Sawa A, Ross CA, Snyder SH. Autophagosome-like vacuole formation in Huntington's disease lymphoblasts. *Neuroreport* 2004; 15**(8)**: 1325-8
28. Sun Z, Runne C, Tang X, Lin F, Chen S. The Gβ3 splice variant associated with the C825T gene polymorphism is an unstable and functionally inactive protein. *Cell Signal*. 2012 Dec; **24**(12): 2349-59.
29. Saini DK, Karunarathne WK, Angaswamy N, Saini D, Cho JH, Kalyanaraman V et al. Regulation of Golgi structure and secretion by receptor-induced G protein βγ complex translocation. *Proc Natl Acad Sci USA* 2010; **107**(25): 11417-22.
30. Rehm A, Ploegh HL. Assembly and intracellular targeting of the betagamma subunits of heterotrimeric G proteins. *J Cell Biol* 1997; **137**(2): 305-317.
31. Werry TD, Wilkinson GF, Willars GB. Mechanisms of cross-talk between G-protein-coupled receptors resulting in enhanced release of intracellular Ca^{2+}. *Biochem. J* 2003; **74**(Pt 2): 281-96.
32. Chan AS, Wong YH. Gbetagamma signaling and Ca2+ mobilization co-operate synergistically in a Sos and Rac-dependent manner in the activation of JNK by Gq-coupled receptors. *Cell Signal* 2004; **16**(7): 823-36.
33. Kong KC, Billington CK, Gandhi U, Panettieri RA Jr, Penn RB. Cooperative mitogenic signaling by G protein-coupled receptors and growth factors is dependent on G(q/11). *FASEB J* 2006; **20**(9): 1558-60.
34. Price DJ, Grove JR, Calvo V, Avruch J, Bierer BE. Rapamycin-induced inhibition of the 70-kilodalton S6 protein kinase. *Science* 1992; **257**(5072): 973–977.
35. Galbaugh T, Cerrito MG, Jose CC, Cutler ML. EGF induced activation of AKT results in mTOR-dependent p70S6 kinase

phosphorylation and inhibition of HC11 cell lactogenic differentiation. *BMC Cell Biol* 2006; (7): 34.
36. Tran H, Brunet A, Griffith EC, Greenberg ME. The many forks in Foxo's road. *Sci STKE* 2003; **2003**(172): RE5.
37. Maruko T, Nakahara T, Sakamoto K, Saito M, Sugimoto N, Takuwa Y et al. Involvement of the bg subunits of G proteins in the cAMP response induced by stimulation of the histamine H1 receptor. *Naunyn Schmiedebergs Arch Pharmacol* 2005; **372**(2): 153-9.
38. Gill A, Hammes SR. Gβγ signaling reduces intracellular cAMP to promote meiotic progression in mouse oocytes. *Steroids* 2007; **72**(2): 117-23.
39. Dumaz N, Marais R. Protein kinase A blocks Raf-1 activity by stimulating14-3-3 binding and blocking Raf-1 interaction with Ras. *J Biol Chem* 2003; **278**(32): 29819-23.
40. Head BP, Patel HH, Roth DM, Murray F, Swaney JS, Niesman IR et al. Microtubules and actin microfilaments regulate lipid raft/ caveolae localisation of adenylyl cyclase signaling components. *J Biol Chem* 2006; **281**(36): 26391-9.
41. Shajahan AN, Tiruppathi C, Smrcka AV, Malik AB, Minshall RD. Gβγ activation of Src induces caveolae-mediated endocytosis in endothelial cells. *J Biol Chem* 2004; **279**(46): 48055-62.
42. Van den Heuvel AP, Schulze A, Burgering BM. Direct control of caveolin-1 expression by Foxo transcription factors. *Biochem J* 2005; **385**(Pt 3): 795-802.
43. Yamamoto M, Okumura S, Oka N, Schwencke C, Ishikawa Y. Downregulation of caveolin expression by cAMP signal. *Life Sci*. 1999; **64**(15): 1349-57.
44. Gao X, Lowry PR, Zhou X, Depry C, Wei Z, Wong GW et al. PI3K/AKT signaling requires spatial compartmentalization in plasma membrane microdomains. *Proc Natl Acad Sci U S A* 2011; **108**(35): 14509-14.
45. Pollard TD, Borisy GG. Cellular motility driven by assembly and disassembly of actin filaments. Cell. 2003; **112**(4): 453-65.
46. Stahlhut M, van Deurs B. Identification of filamin as a novel ligand for caveolin-1: evidence for the organization of caveolin-1-associated membrane domains by the actin cytoskeleton. *Mol Biol Cell* 2000; **11**(1): 325–337.
47. Li Z, Hannigan M, Mo Z, Liu B, Lu W, Wu Y et al. Directional sensing requires G beta gamma-mediated PAK1 and PIX alpha-dependent activation of Cdc42. *Cell* 2003; **114**(2): 215-27.
48. Sasaki AT, Janetopoulos C, Lee S, Charest PG, Takeda K, Sundheimer LW et al. G protein-independent Ras/PI3K/F-actin circuit regulates basic cell motility. *J Cell Biol.* 2007; **178**(2): 185-91.
49. Bulloj A, Duan W, Finnemann SC. PI 3-kinase independent role for AKT in F-actin regulation during outer segment phagocytosis by RPE cells. *Exp Eye Res* 2013; **113**(9-18).
50. Qian Y, Corum L, Meng Q, Blenis J, Zheng JZ, Shi X et al. PI3K induced actin filament remodeling through Akt and p70S6K1: implication of essential role in cell migration. Am J Physiol Cell Physiol. 2004; **286**(1): C153-63.
51. Urra H, Torres VA, Ortiz RJ, Lobos L, Díaz MI, Díaz N et al. Caveolin-1-enhanced motility and focal adhesion turnover require tyrosine-14 but not accumulation to the rear in metastatic cancer cells. *PLoS One* 2012; **7**(4): e33085.
52. Zhou HY, Wong AS. Activation of p70S6K induces expression of matrix metalloproteinase 9 associated with hepatocyte growth factor-mediated invasion in human ovarian cancer cells. *Endocrinology* 2006; **147**(5): 2557-66.
53. Storz P, Döppler H, Copland JA, Simpson KJ, Toker A. Foxo3a promotes tumorcell invasion through the induction of matrix metalloproteinases. *Mol Cell Biol* 2009; **29**(18): 4906-17.
54. Rybkin II, Cross ME, McReynolds EM, Lin RZ, Ballou LM. alpha(1A) adrenergic receptor induces eukaryotic initiation factor 4E-binding protein 1 phosphorylation via a Ca(2+)-dependent pathway independent of phosphatidylinositol 3-kinase/AKT. *J Biol Chem* 2000; **275**(8): 5460-5.
55. Conus NM, Hemmings BA, Pearson RB. Differential regulation by calcium reveals distinct signaling requirements for the activation of AKT and p70S6k. *J Biol Chem* 1998; **273**(8): 4776-82.
56. Cohen JD, Gard JM, Nagle RB, Dietrich JD, Monks TJ, Lau SS. ERK crosstalks with 4EBP1 to activate cyclin D1 translation during quinol-thioether-induced tuberous sclerosis renal cell carcinoma. *Toxicol. Sci.* 2011; **124**(1): 75-87.
57. Koch WJ, Hawes BE, Inglese J, Luttrell LM, Lefkowitz RJ. Cellular expression of the carboxyl terminus of a G protein-coupled receptor kinase attenuates Gβγ-mediated signaling. *J Biol Chem.* 1994; **269**(8): 6193-7.
58. Hall A. Rho GTPases and the actin cytoskeleton. *Science* 1998; **279**(5350): 509-14.
59. Masiero L, Lapidos KA, Ambudkar I, Kohn EC. Regulation of the RhoA pathway in human endothelial cell spreading on type IV collagen: role of calcium influx. *J Cell Sci* 1995; **112**(Pt 19): 3205-13.
60. Sun CX, Downey GP, Zhu F, Koh AL, Thang H, Glogauer M. Rac1 is the small GTPase responsible for regulating the neutrophil chemotaxis compass. *Blood* 2004; **104**(12): 3758-65.
61. Thomas S, Overdevest JB, Nitz MD, Williams PD, Owens CR, Sanchez-Carbayo M et al. Src and caveolin-1 reciprocally regulate metastasis via a common downstream signaling pathway in bladder cancer. *Cancer Res* 2011; **71**(3): 832-41.
62. Reyland ME. Protein kinase C isoforms: Multi-functional regulators of cell life and death. *Front Biosci* 2009; **1**(14): 2386-99.
63. Ren B, Deng Y, Mukhopadhyay A, Lanahan AA, Zhuang ZW, Moodie KL et al. ERK1/2-AKT1 crosstalk regulates arteriogenesis in mice and zebrafish. *J Clin Invest* 2010; **120***(*4): 1217-28.
64. Kageyama K, Ihara Y, Goto S, Urata Y, Toda G, Yano K et al. Overexpression of calreticulin modulates protein kinase B/AKT signaling to promote apoptosis during cardiac differentiation of cardiomyoblast H9c2 cells. *J Biol Chem* 2002; **277**(22): 19255-64.
65. Yasuoka C, Ihara Y, Ikeda S, Miyahara Y, Kondo T, Kohno S. Antiapoptotic activity of AKT is down-regulated by Ca^{2+} in myocardiac H9c2 cells. Evidence of Ca(2+)-dependent regulation of protein phosphatase 2Ac. *J Biol Chem* 2004; **279**(49): 51182-92.
66. Ellis IR, Schor AM, Schor SL. EGF AND TGF-alpha mitogenic activities are mediated by the EGF receptor via distinct matrix-dependent mechanisms. *Exp Cell Res* 2007; **313**(4): 732-41.
67. Thomas CC, Deak M, Alessi DR, van Aalten DM. High-resolution structure of the pleckstrin homology domain of protein kinase b/ AKT bound to phosphatidylinositol (3,4,5)-trisphosphate. *Curr Biol* 2002; **12**(14): 1256–1262.
68. Yoeli-Lerner M, Yiu GK, Rabinovitz I, Erhardt P, Jauliac S, Toker AAKT blocks breast cancer cell motility and invasion through the transcription factor NFAT. *Mol Cell* 2005; **20**(4): 539–550.
69. Liu H, Radisky DC, Nelson CM, Zhang H, Fata JE, Roth RA et al. Mechanism of AKT1 inhibition of breast cancer cell invasion reveals a protumorigenic role for TSC2. *Proc Natl Acad Sci USA* 2006; **103**(11): 4134–4139.
70. Irie HY, Pearline RV, Grueneberg D, Hsia M, Ravichandran P, Kothari N et al. Distinct roles of AKT1 and AKT2 in regulating cell migration and epithelial-mesenchymal transition. *J Cell Biol* 2005; **171**(6): 1023–1034.
71. Ellis IR, Jones SJ, Lindsay Y, Ohe G, Schor AM, Schor SL et al. Migration Stimulating Factor (MSF) promotes fibroblast migration by inhibiting AKT. *Cell Signal* 2010; **22**(11): 1655-9.
72. Zhao J, Brault JJ, Schild A, Cao P, Sandri M, Schiaffino S et al. Foxo3 coordinately activates protein degradation by the autophagic/lysosomal and proteasomal pathways in atrophying muscle cells. *Cell Metab* 2007; **6**(6): 472-83.
73. Kim BW, Choi M, Kim YS, Park H, Lee HR, Yun CO et al. Vascular endothelial growth factor (VEGF) signaling regulates hippocampal neurons by elevation of intracellular calcium and activation of calcium/calmodulin protein kinase II and mammalian target of rapamycin. *Cell Signal* 2008; **20**(4): 714-25.

74. Du M, Shen QW, Zhu MJ, Ford SP. Leucine stimulates mammalian target of rapamycin signaling in C2C12 myoblasts in part through inhibition of adenosine monophosphate-activated protein kinase. *J Anim Sci* 2007; **85**(4): 919-27.
75. Beugnet A, Wang X, Proud CG. Target of rapamycin (TOR)-signaling and RAIP motifs play distinct roles in the mammalian TOR-dependent phosphorylation of initiation factor 4E-binding protein 1. *J Biol Chem* 2003; **278**(42): 40717-22.
76. Iijima Y, Laser M, Shiraishi H, Willey CD, Sundaravadivel B, Xu L et al. c-Raf/MEK/ERK pathway controls protein kinase C-mediated p70S6K activation in adult cardiac muscle cells. *J Biol Chem* 2002; **277**(25): 23065-75.
77. Gu M, Lynch J., Brecher P. Nitric oxide increases p21(Waf1/Cip1) expression by a cGMP-dependent pathway that includes activation of extracellular signal-regulated kinase and p70(S6k). *J Biol Chem* 2002; **275**(15): 11389–11396.
78. Whelan MC, Senger DR. Collagen I initiates endothelial cell morphogenesis by inducing actin polymerization through suppression of cyclic AMP and protein kinase A. *J Biol Chem* 2003; **278**(1): 327–334.
79. Ip CKM, Cheung ANY, Ngan HYS, Wong AST. p70 S6 kinase in the control of actin cytoskeleton dynamics and directed migration of ovarian cancer cells. *Oncogene* 2011; **30**(21): 2420-32.
80. Beardsley A, Fang K, Mertz H, Castranova V, Friend S, Liu J. Loss of caveolin-1 polarity impedes endothelial cell polarization and directional movement. *J Biol Chem*. 2005; **280**(5): 3541-7.
81. Santilman V, Baran J, Anand-Apte B, Evans RM, Parat MO. Caveolin-1 polarization in transmigrating endothelial cells requires binding to intermediate filaments. *Angiogenesis* 2007; **10**(4): 297-305.
82. Patel HH, Murray F, Insel PA. Caveolae as organizers of pharmacologically relevant signal transduction molecules. *Annu Rev Pharmacol Toxicol* 2008; 48:359-91.
83. Waschke J, Curry FE, Adamson RH, Drenckhahn D. Regulation of actin dynamics is critical for endothelial barrier functions. *Am J Physiol Heart Circ Physiol* 2005; **288**(3): H1296-305.
84. Seko T, Ito M, Kureishi Y, Okamoto R, Moriki N, Onishi K et al. Activation of RhoA and inhibition of myosin phosphatase as important components in hypertension in vascular smooth muscle. *Circ Res* 2003; **92**(4): 411-8.
85. Emamghoreishi M, Schlichter L, Li PP, Parikh S, Sen J, Kamble A et al. High intracellular calcium concentrations in transformed lymphoblasts from subjects with bipolar I disorder. *Am J Psychiatry* 1997; **154**(7): 976-82.
86. Newton R, Cambridge L, Hart LA, Stevens DA, Lindsay MA, Barnes PJ. The MAP kinase inhibitors, PD098059, UO126 and SB203580, inhibit IL-1beta-dependent PGE(2) release via mechanistically distinct processes. *Br J Pharmacol* 2000; **130**(6): 1353-61.
87. Dang VC, Napier IA, Christie MJ. Two distinct mechanisms mediate acute μ-opioid receptor desensitization in native neurons. *J Neurosci* 2009; **29**(10): 3322-7.